Evaluation Results of US-APWR Fuel System Structural Response to Seismic and LOCA Loads

Non-Proprietary Version

March 2009

Revision History

Revision	Page	Description
0	All	Original Issue

Mitsubishi Heavy Industries, Ltd.
16-5, Konan 2-chome, Minato-ku
Tokyo 108-8215 Japan

Abstract

During a seismic event, the reactor vessel is accelerated laterally and vertically and these accelerations are transmitted to the fuel assemblies via the reactor internal structures, such as the upper core plate and the lower core support plate. The fuel assemblies respond laterally and vertically due to these accelerations. The loss of coolant event (LOCA) can also result in a significant fuel assembly dynamic response due to the LOCA-specific accelerations and transient flow in the core. The same type of analysis input parameters and modeling applies to the evaluation of the effects of both seismic and LOCA events.

In accordance with Standard Review Plan Section 4.2 (NUREG-0800), each fuel assembly and the core must be designed to maintain a coolable geometry and allow safe shutdown of the reactor during both seismic and LOCA events. The fuel assembly will be shown to satisfy the SRP guidelines by specific stress criteria and component deformation limits. The rod cluster control assembly (RCCA) will be shown to maintain its integrity by satisfying stress limits to provide a safe shutdown of the reactor. This document describes the evaluation method and provides the results which show that the SRP requirements are met.

The document also describes the effects of irradiation on the fuel assembly's structure and dynamic response as the integrity of the fuel assembly may be affected during seismic and LOCA events.

Table of Contents

List of Tables

List of Figures

1.0 INTRODUCTION

The US-APWR fuel assembly (referred to simply as 'fuel assembly' below), is an important structural component of the core. The array of fuel assemblies is contained by a core support structure placed within the reactor vessel, and during operation is subject to coolant flow at high temperature and pressure. With respect to the Standard Review Plan, Section 4.2 (NUREG-0800) [1-1], the fuel assembly must be able to maintain core coolability (coolable geometry) and the control rod insertion for safe reactor shutdown during both seismic and loss of coolant accident (LOCA) events. The fuel assembly must be designed to fulfill those functions.

The US-APWR rod control cluster assembly (referred to simply as 'RCCA' below) is also an important structural component of the core. It is almost fully withdrawn from the fuel assembly during normal operation, but needs to be inserted rapidly into the fuel assembly to shut down the reactor. The RCCAs must be designed to maintain their insertion function during seismic and LOCA events.

Based on Reference 1-2, this report describes the functional requirements for the fuel assembly and the RCCA, the design philosophy, the acceptance criteria, the evaluation methodologies to demonstrate that the functional requirements for the fuel assembly and the rod cluster control assembly are maintained in the seismic and LOCA conditions, and the evaluation results.

This report also describes the effects of irradiation on the fuel assembly's structure and dynamic response as the integrity of the fuel assembly may be affected during seismic and LOCA events.

References

(1-1) U.S. Nuclear Regulatory Commission, Standard Review Plan (NUREG-0800) Section 4.2, March 2007

(1-2) "Mitsubishi Fuel Design Criteria and Methodology", MUAP-07008-P (Proprietary) and MUAP-07008-NP (Non-Proprietary), May 2007

2.0 DESCRIPTION, FUNCTIONAL REQUIREMENTS AND ACCEPTANCE CRITERIA FOR THE FUEL ASSEMBLY AND ROD CLUSTER CONTROL ASSEMBLY

2.1. Description of the Fuel Assembly and Rod Cluster Control Assembly

The structure of the US-APWR fuel assembly is shown in Figure 2.1-1. The fuel assembly is comprised of a 17 x 17 square array of 264 fuel rods, 24 control rod guide thimbles, and one guide tube for in-core instrumentation, as well as eleven grid spacers, one top nozzle and one bottom nozzle. As shown in Figure 2.1-2, the RCCA consists of one spider and 24 control rods attached to the spider.

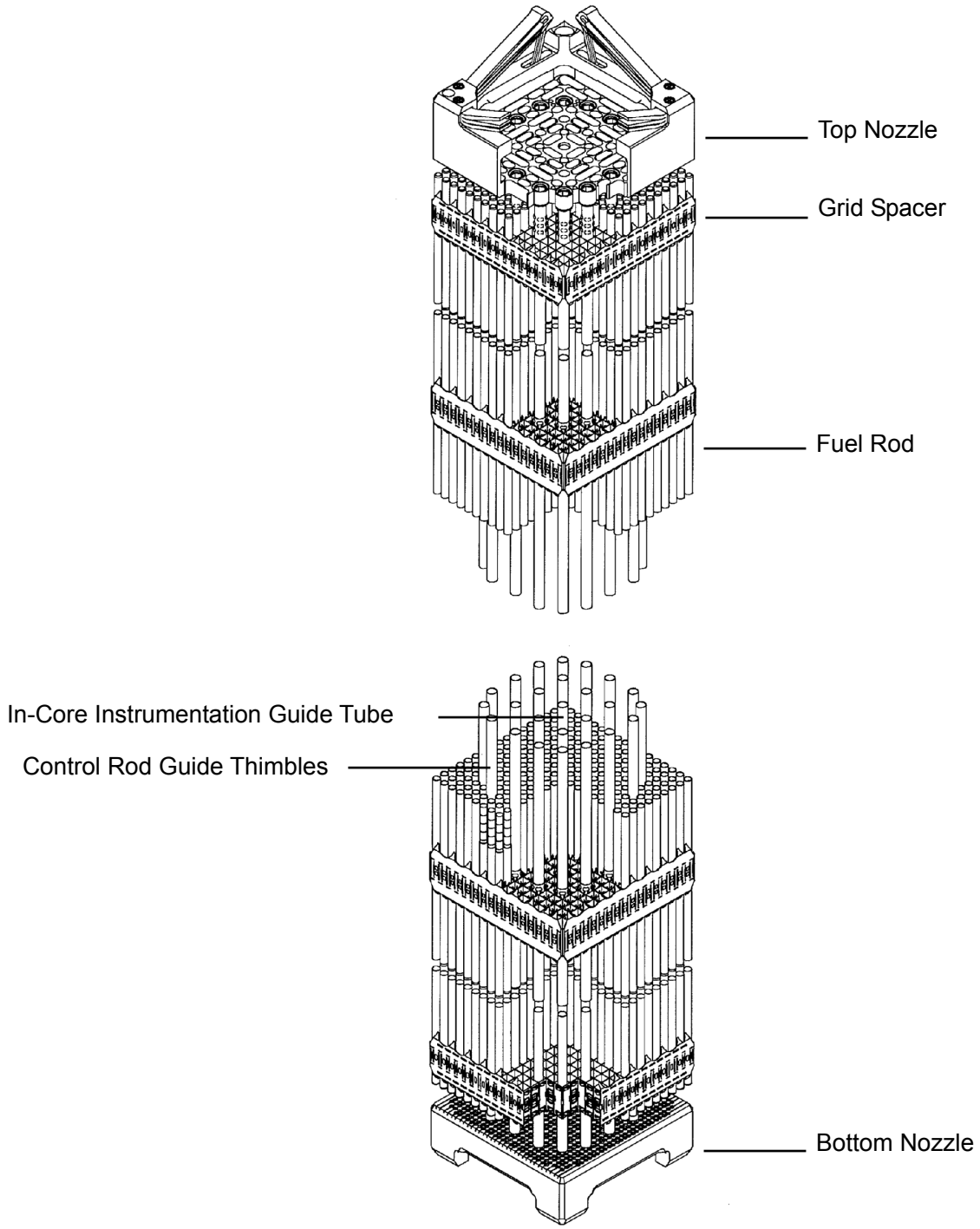

Figure 2.1-1 Structural Schematic for the US-APWR Fuel Assembly

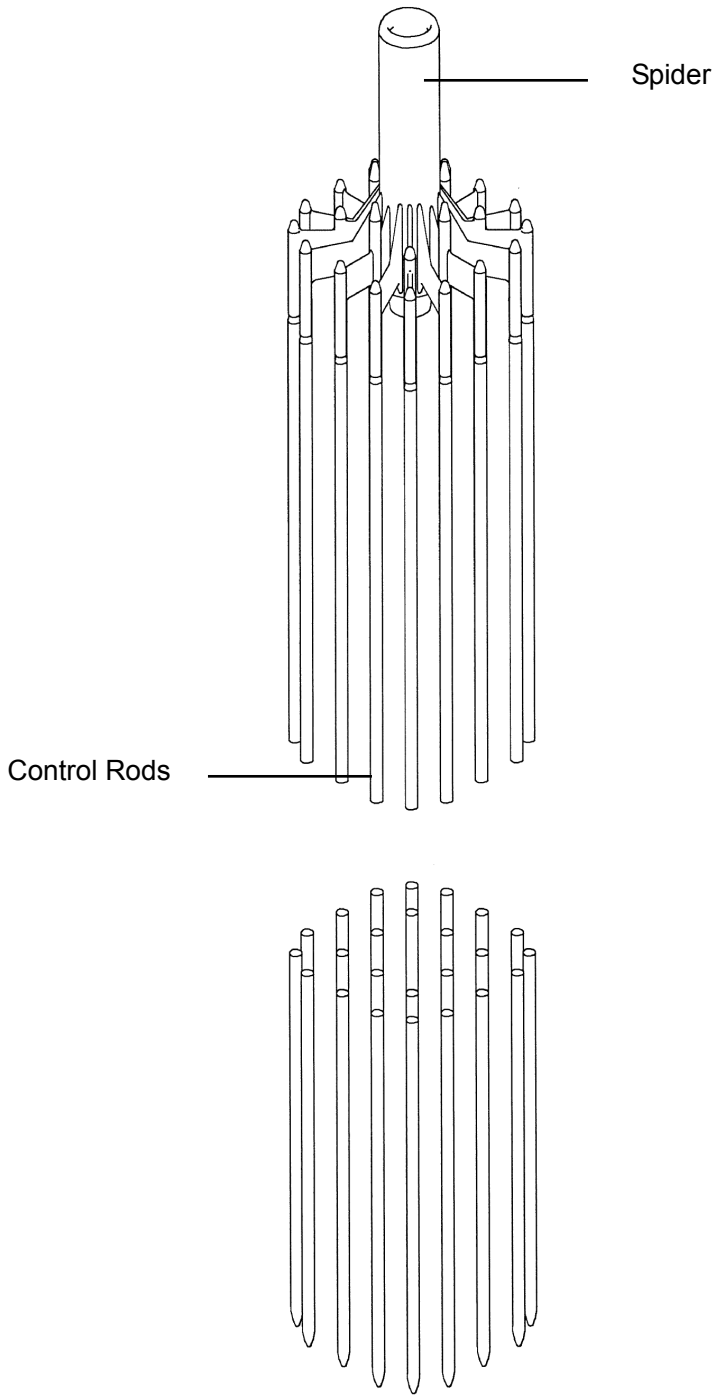

Figure 2.1-2 Structural Schematic for the US-APWR Rod Cluster Control Assembly

2.2. Functional Requirements for the Fuel Assembly and the Rod Cluster Control Assembly

In Section 3.7.1 of Reference 2-1, it is stated that the Operating Basis Earthquake (OBE) accelerations are assumed to be limited to 1/3 of the Safe Shutdown Earthquake (SSE) accelerations and therefore, in accordance with Appendix S of 10 CFR 50[(2-2)], it is not required to perform an explicit response or design analysis for the OBE.

The evaluation for the fuel assembly and the RCCA during an SSE event is described in this report. The functional requirements for the fuel assembly and the rod cluster control assembly during an SSE are described in this section and in Reference 2-3.

In accordance with SRP Section 4.2 [(2-4)], the fuel assembly and the RCCA must be designed to maintain a coolable geometry of the core and maintain control rod insertion function to shut down the reactor safely during both Safe Shutdown Earthquake and LOCA events. The safety functions of the US-APWR fuel assembly and the RCCA components, to ensure this capability, are listed in Table 2.2-1.

Table 2.2-1 Functional Requirements for the Fuel Assembly and Rod Cluster Control Assembly

Component	Functional Requirements	Comments
Grid spacers, top and bottom nozzles	Maintaining coolable geometry of the core	Maintain adequate fuel rod spacing to prevent major damage to the fuel cladding.
Control rod guide thimbles	Maintaining coolable geometry of the core	Structurally connects the top and bottom nozzles and the grid spacers to maintain the fuel assembly and core shape by supporting the fuel rods via the grid spacers.
	Safe reactor shutdown	Maintain an adequate path for insertion of the RCCA into the fuel assembly.
Fuel cladding	Maintaining coolable geometry of the core	Fuel cladding fragmentation must not occur.
Control rod cladding and top end plug	Safe reactor shutdown	Maintain geometry of RCCA to allow insertion of control rods into the fuel assembly.

2.3. Design Philosophy and Acceptance Criteria

To maintain the functions listed in Table 2.2-1, each component must be designed to have the required strength.

There are, however, no specific acceptance criteria regarding the strength requirements for these components during a seismic and LOCA event in the ASME Code Section III [2-5] or SRP Section 4.2 [2-4] except for fuel cladding. Therefore, the basis for the acceptance criteria defined in the ASME Code Section III Subsection NG [2-5] for core support structures, which have the same safety functions as the fuel assembly and the RCCA, will be applied to these components.

For the control rod guide thimbles, an acceptance criterion related to buckling under vertical load is included to assure that the effects of this deformation mechanism will not interfere with control rod insertion. For the grid spacers, which maintain the spacing of the control rod guide thimbles and fuel rods, there are additional acceptance criteria with regard to maintaining the coolable geometry of the core.

The specific acceptance criteria are presented in Table 2.3-1.

Table 2.3-1 Acceptance Criteria for Safe Shutdown Earthquake and LOCA

Structural Component	Acceptance Criteria	
	Primary General Membrane Stress	Primary Membrane Stress + Primary Bending Stress
Control Rod Guide Thimble Top and Bottom Nozzles	Min. (2.4 Sm, 2/3 Su) *	Min. (3.6 Sm, Su)
Grid Spacer	No excessive deformation shall occur due to load during an accident	
Fuel Cladding	90% of the irradiated yield stress at the appropriate temperature	
Control Rod Guide Thimble	Shall not buckle when subjected to vertical compressive load during an accident	
Cladding and top end plug of control rod	Min. (2.4 Sm, 2/3 Su)	Min. (3.6 Sm, Su)

* Sm is the allowable stress intensity value; Su is ultimate tensile stress.

2.4. References

(2-1) "US-APWR Design Control Document", MUAP-CD003 Revision 1, August 2008

(2-2) Earthquake Engineering Criteria for Nuclear Power Plants, Domestic Licensing of Production and Utilization Facilities, Energy. Title 10 Code of Federal Regulations Part 50, Appendix S, Part IV(a)(1)(i), U.S. Nuclear Regulatory Commission, Washington, DC.

(2-3) "Mitsubishi Fuel Design Criteria and Methodology", MUAP-07008-P (Proprietary) and MUAP-07008-NP (Non-Proprietary), May 2007

(2-4) U.S. Nuclear Regulatory Commission, Standard Review Plan (NUREG-0800) Section 4.2, March 2007

(2-5) American Society of Mechanical Engineers Boiler and Pressure Vessel Code Section III

3.0 BOUNDARY CONDITIONS OF THE FUEL ASSEMBLY AND THE ROD CLUSTER CONTROL ASSEMBLY FOR SEISMIC AND LOCA

3.1. Structures Interacting with the Fuel Assembly and the Rod Cluster Control Assembly and Resultant Loads

The fuel assembly is placed inside the reactor vessel as shown in Figure 3.1-1. The reactor vessel also contains structures that support the fuel assemblies, guide the control rods, and form paths for coolant flow. The upper core plate, the lower core support plate, the core support columns, and other such structures that support the fuel assemblies are referred to as the core support structures. The fuel assembly is supported within the core barrel by the upper core plate and the lower core support plate, and is laterally positioned by pins attached to the upper core plate and the lower core support plate. It is also surrounded by neutron reflector plates that constrain the periphery of the core.

During normal operating conditions, the RCCA drive rod is engaged with the control rod drive mechanism (CRDM) at about its mid-point and with the RCCA spider hub at its bottom. The drive rod and RCCA spider/rods are supported laterally, above the upper core plate by a series of guide plates within the upper internals guide columns when the RCCA is withdrawn from the fuel assembly. Only the tip of the control rod is in the fuel assembly during normal operation.

During normal reactor operation, the hydraulic lift force, gravity and buoyant force act on the fuel assembly in addition to the mechanical force from the fuel assembly holddown springs to prevent liftoff of the fuel assembly. During a seismic event, the motion of the reactor vessel results in loads on the fuel assembly. During a LOCA event pressure fluctuations and hydraulic flow fluctuations occur in the reactor vessel which result in reactor internals motion and loads on the fuel assemblies.

For the RCCA, the vibration of the reactor vessel due to a seismic event is transmitted to the RCCA by way of the upper internals guide column's guide plates. When a LOCA occurs, the loads that accompany pressure fluctuations and hydraulic flow fluctuations in the reactor vessel act on the RCCA. The motions of the RCCA during a seismic or LOCA event must not prevent safe shutdown of the reactor.

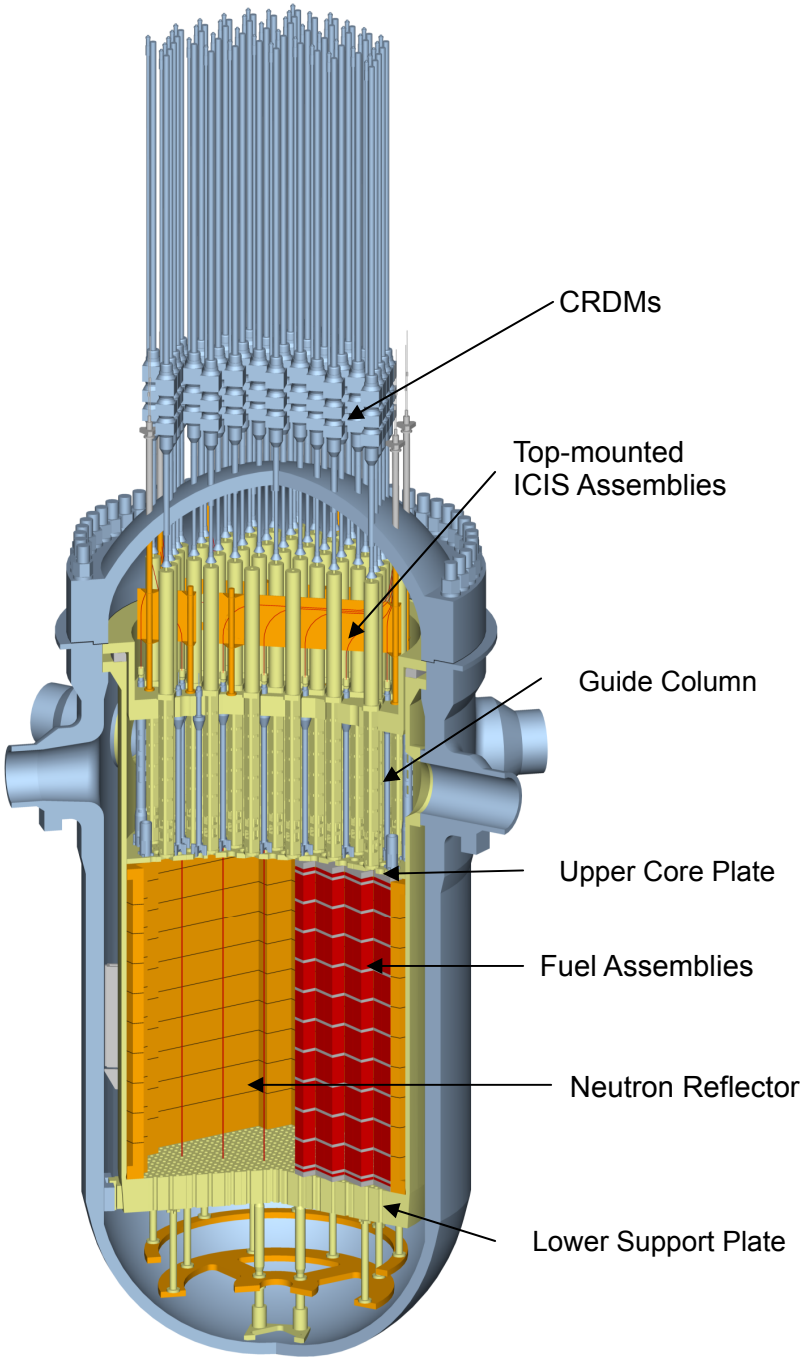

Figure 3.1-1 US-APWR Reactor Vessel Structures

3.2. Behavior of the Fuel Assembly and Rod Cluster Control Assembly for Seismic Conditions

The source of vibration and resultant loads on the fuel assembly and the RCCA during a seismic event are described below.

3.2.1 Fuel Assembly

- The seismic event starts with the ground motion (accelerations) resulting in vibration of the reactor building which leads to the vibration of the reactor vessel.
- The vibration of the reactor vessel is accompanied by vibration of the upper core plate and the lower core support plate that support the ends of the fuel assemblies.
- The upper core and the lower core support plates vibrate in both the vertical and horizontal directions, resulting in vibration of the fuel assemblies supported by the plates. The neutron reflector plates act as rigid beams with the top and bottom ends connected/moving with the upper core plate and lower core support plate, respectively.
- The magnitude and phase of the acceleration that act on every fuel assembly (through the upper core plate and lower core support plate core pins) are the same due to the horizontal rigidity of the upper core and lower core support plates. Therefore, the ends of all fuel assemblies move synchronously. If the vibration is large the displacement of the outermost fuel assemblies is limited by the neutron reflector or the gap between adjacent assemblies. Therefore collisions may occur with the neutron reflector plates or adjacent fuel assemblies at the grid spacers, which affects the horizontal vibration behavior of each fuel assembly.
- Vertical vibration of the upper core plate and the lower core support plate act on the fuel assembly in the form of a compressive load due to the variation of distance between these plates. If the vertical acceleration of the lower core support plate is large, it may cause the fuel assembly to lift off the lower core support plate and impact back into contact with the lower core support plate. As the transient subsides, the fuel assembly will come back into contact with the lower core support plate in its original alignment.

3.2.2 RCCA

- Vibration of the reactor building caused by the seismic event leads to the vibration of the reactor vessel.
- The vibration of the reactor vessel is accompanied by vibration of the CRDMs and the guide plates in the upper internals guide columns that support the RCCAs.
- The horizontal vibration is transmitted to the RCCAs by way of the guide plates and the vertical vibration is transmitted by way of the CRDMs.
- The horizontal displacement of the RCCA control rod caused by the guide plate vibration is limited by the short span between the guide plates.
- During a scram, the RCCA drops into the fuel assembly while being guided by the guide plates in the guide column and by the fuel assembly guide thimbles. The shape of the portion of the RCCA control rod in the fuel assembly guide thimble is essentially the same as that of the fuel assembly during the seismic event.

3.3. Postulated Accident - LOCA

Of the postulated design basis accidents, LOCA involves a large fluctuation of pressure and hydraulic flow inside the reactor, which result in significant loads on the fuel assembly and the RCCA. In a LOCA caused by failure of a coolant pipe, a decompression wave is generated at the point of failure which envelopes the core barrel vertically and circumferentially. This creates a time differential in the arrival of the decompression wave around the core that gives rise to loads, thus inducing vibration in the core. Therefore, LOCA is chosen as a design limiting event since it can result in significant fuel assembly and RCCA vibration response.

3.4. Behavior of the Fuel Assembly and Rod Cluster Control Assembly for LOCA Conditions

The fuel assembly and the RCCA behavior during LOCA are described below.

3.4.1 Fuel Assembly

- Because the upper core plate and the lower core support plate vibrate in both the horizontal and vertical directions due to the LOCA, the fuel assemblies supported by them are vibrated by the LOCA as well. The neutron reflector plates act as rigid beams with the top and bottom ends connected/moving with the upper core plate and lower core support plate, respectively.
- The horizontal vibration of the upper core and the lower core support plates during LOCA is at the fundamental frequency of the core barrel. Because the primary vibration component is near 10 Hz, the fuel assemblies respond in a tertiary mode near their natural frequency. As with the seismic response in Section 3.2, the magnitude and phase of the acceleration that act on the fuel assemblies due to the vibration of the upper and lower support points are the same, and therefore the ends of all fuel assemblies vibrate synchronously. If the vibration is large, however, the displacement of the outermost fuel assemblies is limited by the neutron reflector or the gap between adjacent assemblies. Therefore collisions may occur with the neutron reflector plates or adjacent fuel assemblies at the position of the grid spacers, which affects the horizontal vibration behavior of each fuel assembly.
- The vertical response of the fuel assembly is analyzed in a similar manner to the seismic event analysis in terms of the internals response, but there are also significant transient axial flow effects that act on the fuel assembly that may cause it to lift off the lower core support plate and impact back into contact with the lower core support plate. As the flow subsides during the LOCA the fuel assembly will come back into contact with the lower core support plate in its original alignment.

3.4.2 RCCA

- The horizontal acceleration is transmitted to the RCCAs by way of the guide plates in the upper internals guide columns and the vertical acceleration is transmitted by way of the CRDMs into the RCCA drive rods.
- As with the seismic response in Section 3.2, the displacement of the RCCA in the horizontal direction caused by the upper internals guide column guide plate vibration is limited by the short span between the guide plates.

- The vertical acceleration of the CRDM results in axial stresses in the control rod cladding, the control rod top end plug, and the RCCA spider assembly components.
- During a scram, the RCCA drops into the fuel assembly while being aligned by the guide plates in the guide column and by the fuel assembly guide thimbles. The shape of the portion of the RCCA control rod in the fuel assembly guide thimble is essentially the same as that of the fuel assembly during the LOCA event.

4.0 RESPONSE AND STRESS ANALYSIS OF THE FUEL ASSEMBLY FOR SEISMIC AND LOCA CONDITIONS

4.1. Methodology for the Fuel Assembly Seismic Response and Stress Analysis

4.1.1. Methodology for the Fuel Assembly Seismic Horizontal Response Analysis

4.1.1.1. Procedure for the Fuel Assembly Seismic Horizontal Response Analysis

The fuel assembly horizontal response to an earthquake and LOCA such as displacement of the fuel assembly and impact force at grid spacers among the fuel assemblies and neutron reflectors are independently analyzed by time-dependent response analysis code modeling an array of fuel assemblies. The horizontal displacements obtained are used in the fuel assembly stress analyses. The stress results are combined by the Square Root of the Sum of the Squares (SRSS) method and then compared to the ASME Code allowable stress values.

The process described above is schematically shown in Figure 4.1.1.1-1 [(4-1)].

The FINDS code [(4-2)] is used for the analysis of the fuel assembly horizontal response. The FINDS code was originally developed by MHI for seismic response analysis of an array of fuel assemblies. The vibration model of the fuel assembly in the FINDS is based on empirically-confirmed models for not only the 1st mode response but also higher vibration modes in term of natural frequencies and vibration mode shapes. The deformation characteristics obtained by grid spacer impact tests are included in the model and determine the collision characteristics of the grid spacers.

The FINDS code was verified and validated in compliance with the MHI quality assurance program as described in Appendix D of Reference 4-3.

A time-dependent response analysis is performed on an array of fuel assemblies forming a single row and vibrating along the row. The analytical model for the case with 17 fuel assemblies in a row, the maximum for the US-APWR, is shown in Figure 4.1.1.1-2 [(4-1)]. The individual fuel assembly is modeled with beam elements using the finite element method (FEM). Spring elements that correspond to the stiffness of the grid spacers and damping elements to model rebound characteristics are placed at the grid spacer positions to obtain the collision behavior. Since no collisions occur near the support points at the beam ends, the uppermost and lowermost grid spacers are not included. The upper and lower ends of the beam models are connected to the upper core and the lower core support plates which are modeled as laterally rigid. The neutron reflector located adjacent to the outermost fuel assemblies, is modeled as a rigid wall. The effect of the coolant inside the core is taken into account as an additional mass to the actual mass of the fuel assembly, and the resultant vibration characteristics (the specific frequency of the fuel assembly and the attenuation constant) are used in the analyses.

Due to the input accelerations of the upper core and lower core support plates, displacements of the fuel assembly will occur. In the analysis, the acceleration of the neutron reflector's (acting as rigid beams) top and bottom ends are the same as the accelerations of the upper core plate and the lower core support plate, respectively. Fuel assembly displacements vary according to the magnitude of the input accelerations and by the collisions with adjacent fuel assemblies and with the neutron reflectors. The structures thus exhibit a group vibration behavior.

The fuel assembly response analysis model is two dimensional, as previously shown in Figure 4.1.1.1-2, while the response analysis of the reactor vessel is determined by a 3-dimensional model. Accordingly, the fuel assemblies' response analyses are independently performed using the accelerations in the x and z direction obtained from the reactor internal's response analysis as inputs. The resultant displacements of the fuel assemblies are obtained when the values for the x direction and z direction are combined by the SRSS method.

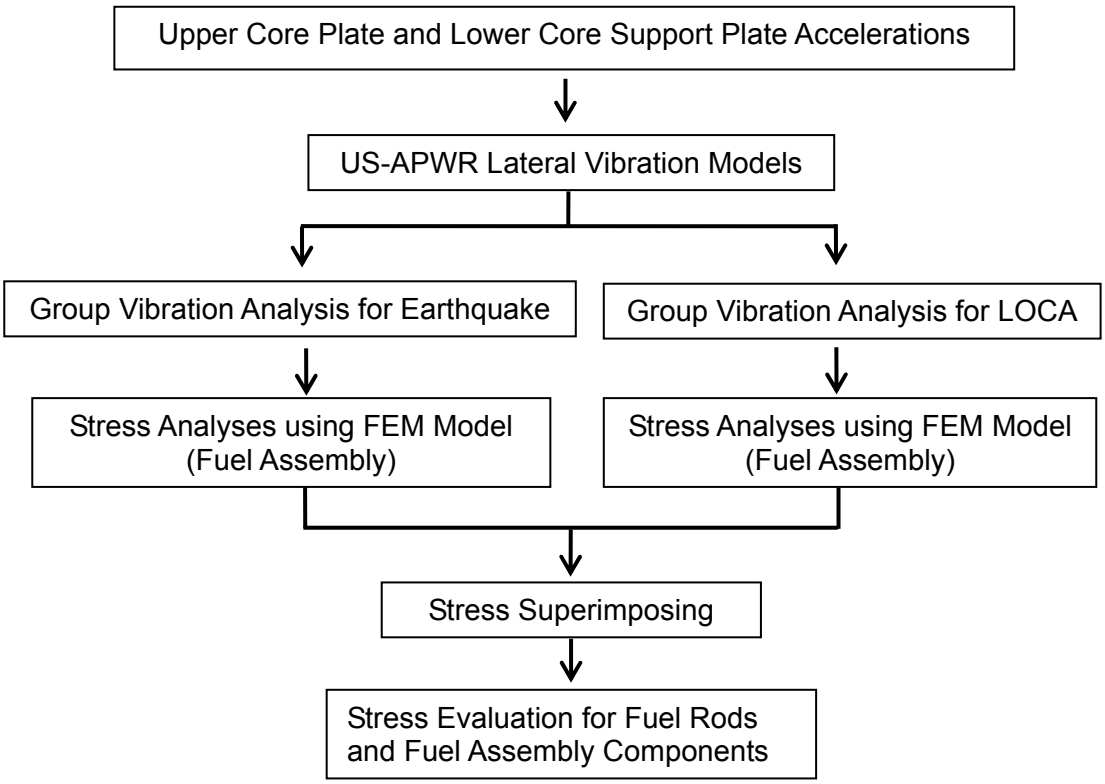

Figure 4.1.1.1-1 Stress Evaluation for Seismic and LOCA Response in the Horizontal Direction

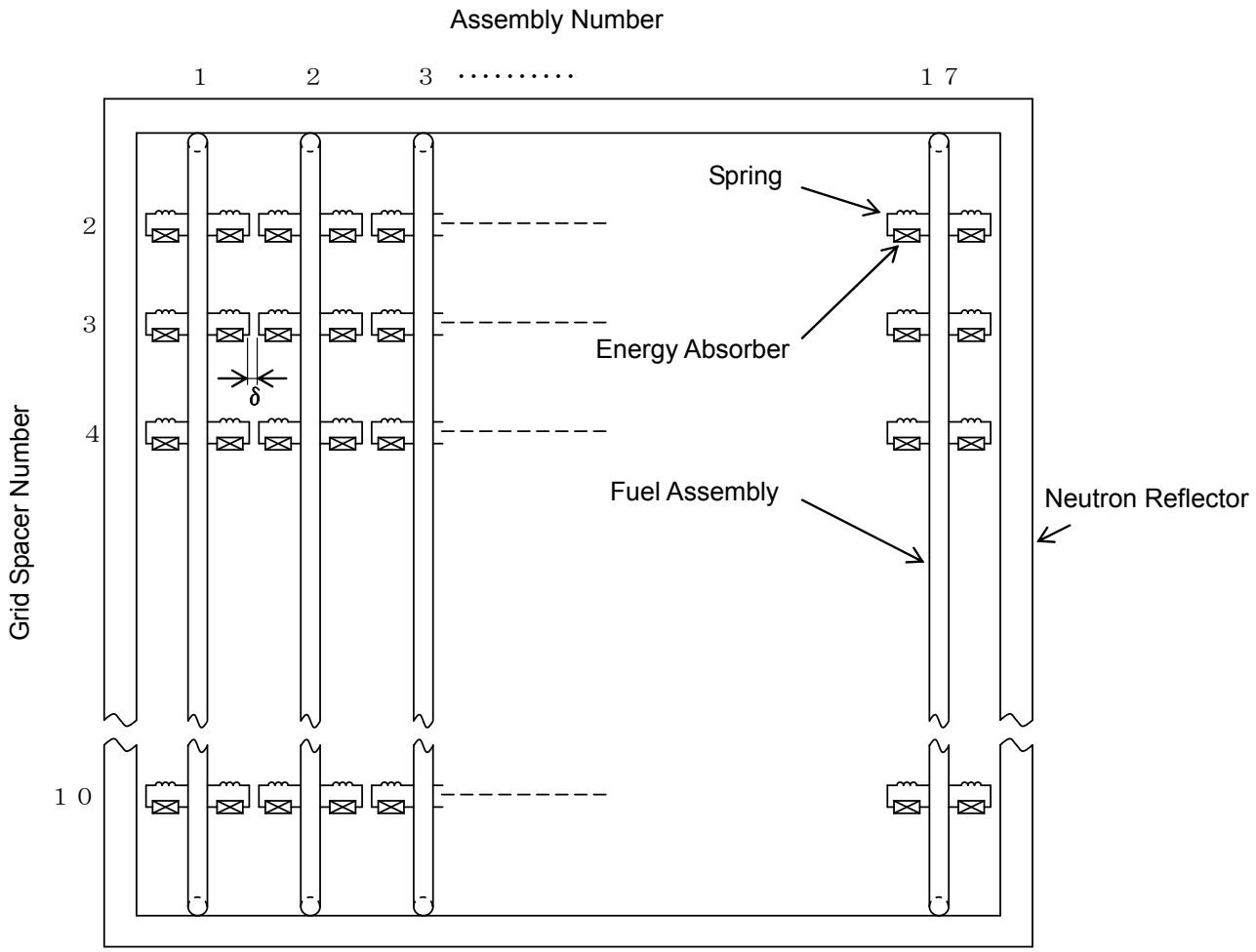

Figure 4.1.1.1-2 Fuel Assembly Vibration Response Analysis Model in the Horizontal Direction

4.1.1.2. Model for the Fuel Assembly Seismic Horizontal Response Analysis

The FINDS code is characterized by its ability to account for the non-linearity of the fuel assembly's vibration characteristics and the grid spacer impact behavior. A description of these behaviors for the as-built 14-ft fuel assembly, used in the FINDS analysis, is described in this section. The effect of irradiation on the fuel assembly's behavior under seismic and LOCA conditions is described in Appendix A of this report.

4.1.1.2.1. Amplitude Dependence of Natural Frequency and Damping Factor

There are strong amplitude dependencies for a PWR fuel assembly, especially for the 1st mode vibrational damping and frequency. These characteristics are due to the contact mechanism between the fuel rods and grid spacers as shown in Figure 4.1.1.2.1-1. Since the fuel rods are axially supported only by the friction interaction with the grid spacers, the axial and lateral slippage and/or the lift-off of fuel rods from the supporting grid spacer springs and dimples becomes increasingly significant as the deflection of the fuel assembly increases. The friction effects result in an energy loss during each vibrational cycle of the fuel assembly, and are a primary cause of the damping variation. The softening of the fuel assembly lateral stiffness at larger deflections is due to a reducing contribution of fuel rod stiffness to the overall fuel assembly stiffness as more rods are slipping. This reduced overall fuel assembly stiffness causes a decrease in the natural frequency.

The amplitude dependence of the natural frequency and damping is considered in the FINDS analysis. The relationship can be determined based on the experiment results from the fuel assembly lateral pluck test or estimated by an ANSYS FEM analysis. Both are described in Appendix A of Reference 4-3.

An analysis model for a 14ft fuel assembly has been developed and the free vibration behavior has been calculated for the cold in-air condition. Figure 4.1.1.2.1-2 shows the analysis results. The FINDS input is set to simulate the characteristics of the cold in-air condition.

Appendix B describes the uncertainty of the FINDS input and the analyses results.

At reactor conditions, the effect of coolant on the vibration characteristics is considered and is estimated as follows.

(1) Natural frequency

The effect of coolant on the natural frequency is considered as an added mass in the model. As is stated in Section 4.3 of Reference 4-2, the effect of the added mass for cold condition is determined from the measured vibration characteristics in air and in cold water. [ ]

According to past test results of the fuel assemblies with a various number of grid spacers, the same method can be applied for the calculation of the added mass in the cold condition, and therefore, its application to the 14ft fuel assembly is appropriate. [ ]

(2) Damping factor

For the 14-ft fuel assembly, as previously mentioned, the damping factor with amplitude dependency in air is calculated by ANSYS with some adjustments due to limitations of the ANSYS analysis, as described in the next paragraph.

The damping factor in air is smaller than for in reactor operating conditions and if used would result in an overly conservative vibration response of the fuel assembly. Therefore, the damping factor during reactor operation used in the FINDS model for the 14-ft fuel assembly is an adjusted value based on the damping factor in-air predicted by ANSYS model for 14-ft fuel assembly, as shown in Figure 4.1.1.2.1-2 (b).

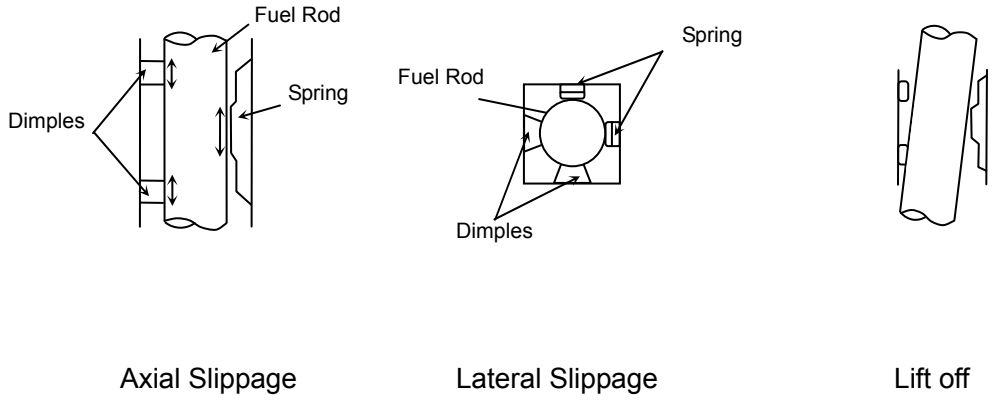

Figure 4.1.1.2.1-1 Non-linear Mechanisms in a Fuel Assembly Structure

frequency(Hz)

amplitude(mm)

(a) Natural Frequency

damping(−)

amplitude(mm)

(b) Damping Factor

Figure 4.1.1.2.1-2 Prediction of Amplitude Dependence of Natural Frequency and Damping Factor in a 14-ft Fuel Assembly (Cold In-Air Condition)

4.1.1.2.2. In-elastic Impact Model for Grid Spacer

In order to solve for the multi-fuel assembly impacting interaction, one grid spacer is modeled by a spring and a damper element pair, located on both sides of the beam because impacting needs to be considered to occur on both sides of the fuel assembly.

When the impact force at the grid spacer exceeds its elastic limit, buckling occurs in one row of grid spacer cells. The buckling may propagate to the next row depending on the impact force generated in later impacts. As mentioned above, semi-empirical rules are used in the FINDS code to express the grid spacer deformation progress. They are derived from the experimental results obtained by the "pendulum and grid spacer" type impact and deformation tests shown in Figure 4.1.1.2.2-1. The in-elastic model for the analysis is adjusted based on the test results for grid spacers with as-built spring force as shown in Figure 4.1.1.2.2-2 for the impact force versus test sequence and 4.1.1.2.2-3 for the plastic deformation versus test sequence. These figures are for test grids identified as As-built_5 and As-built_6 that are the two of six as-built grids impact tested that were used to determine the post-buckling force versus deformation characteristics explained in Appendix A of this report.

The angle of the pendulum during the test sequence for each grid is started at ( ) degrees and increased to a maximum of ( ) degrees as the tests are repeatedly performed. An overlay of the calculated and measured results shows that deformation characteristics are appropriately simulated. Detailed explanations for the impact test and the in-elastic impact model are described in Section A.3.1.1 of Appendix A of this report.

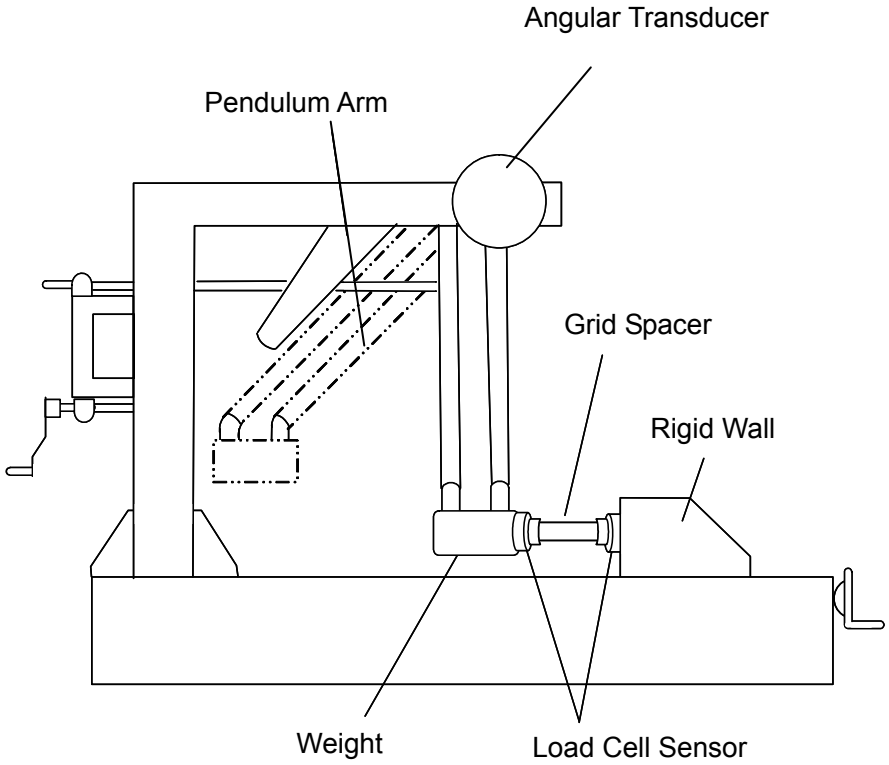

Figure 4.1.1.2.2-1 Grid Spacer and Pendulum Type Impact Test

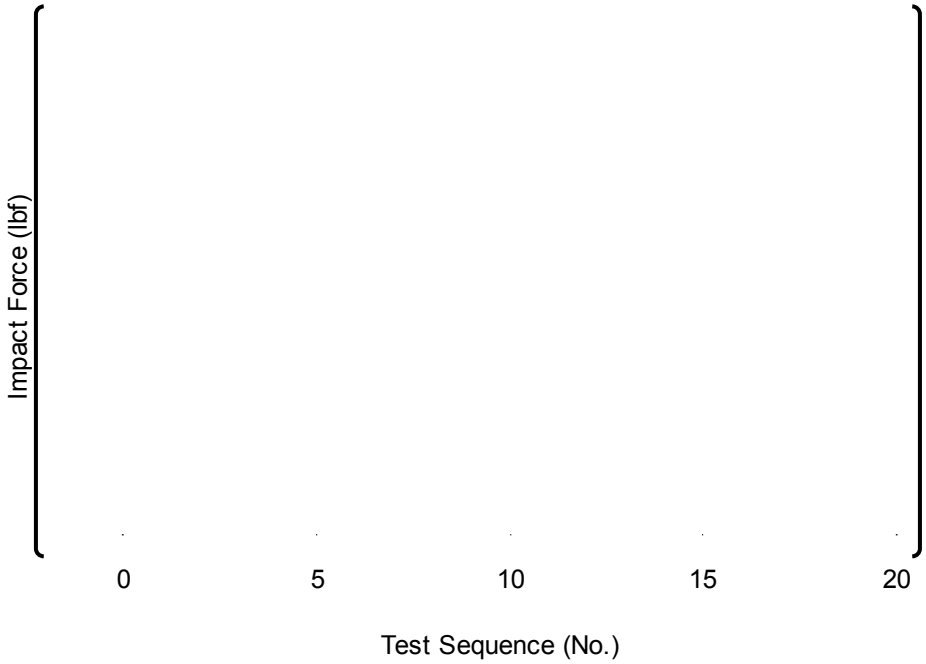

(a) As-Built_5

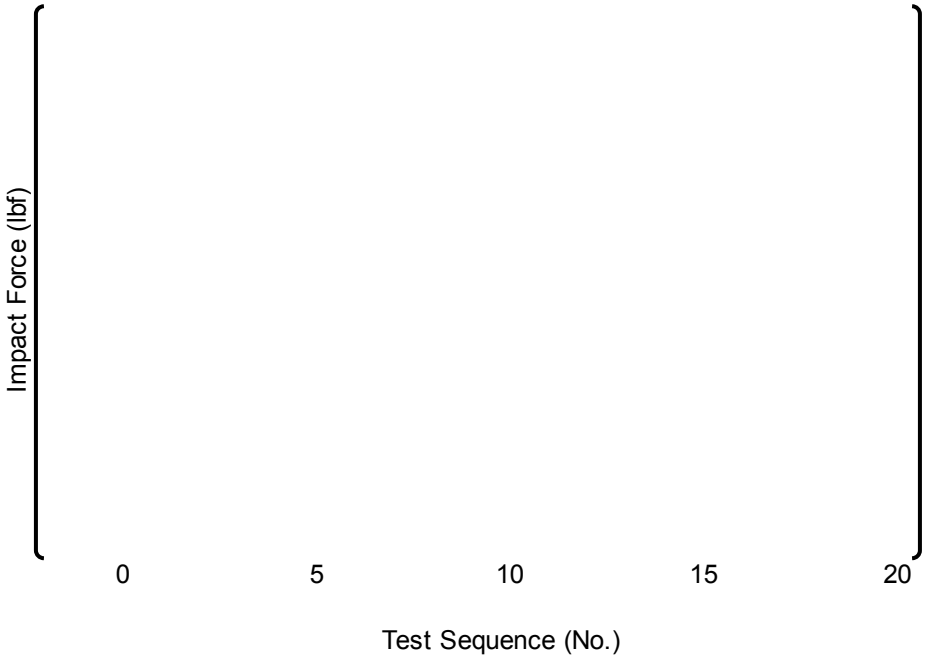

(b) As-Built_6

Figure 4.1.1.2.2-2 Comparison of Analyzed and Measured Impact Force

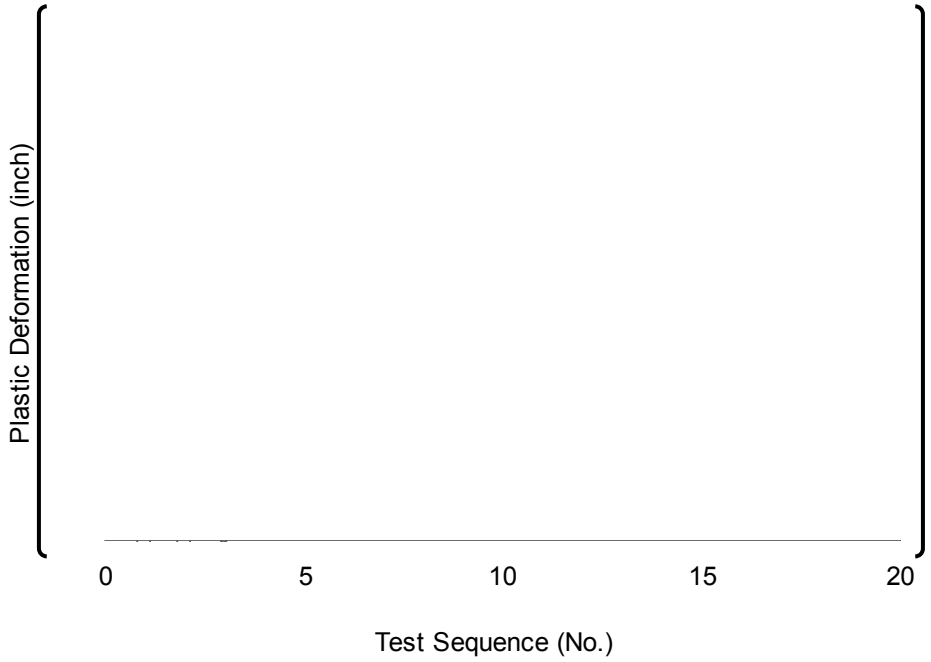

(a) As-Built_5

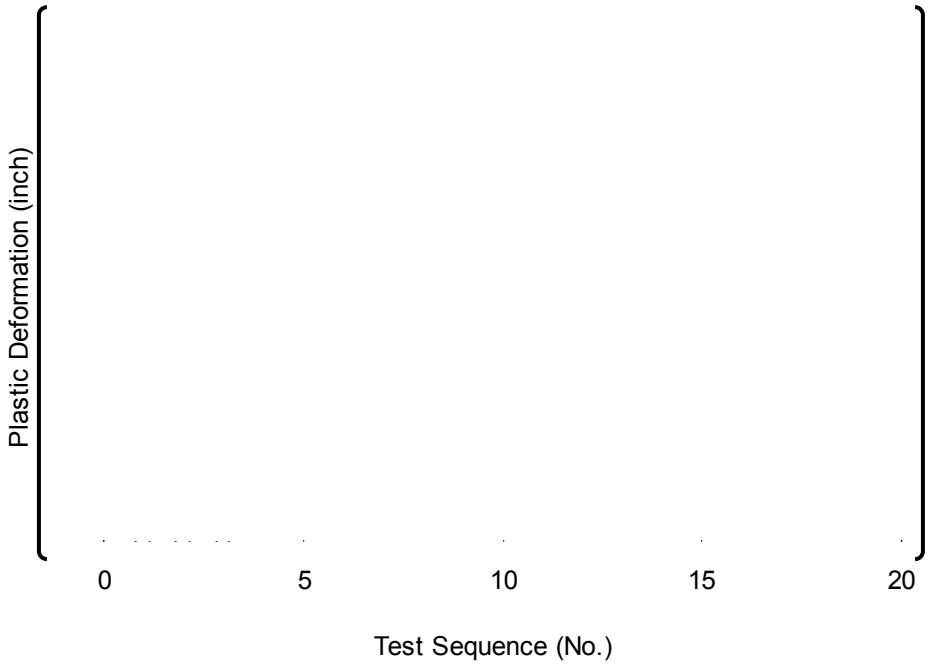

(b) As-Built_6

Figure 4.1.1.2.2-3 Comparison of Analyzed and Measured Plastic Deformation

4.1.2. Methodology for the Fuel Assembly Seismic Horizontal Response Stress Analysis

The fuel assembly stress analysis model in the horizontal direction is shown in Figure 4.1.2-1[4-1]. [ ] The general FEM code ANSYS is used for the analyses.

The stresses due to the fuel assembly horizontal displacement by an earthquake and LOCA are individually analyzed by using the above model. [ ] The stresses in the cladding and the control rod guide thimble resulting from the SSE analysis are combined with those for LOCA by the SRSS method.

Figure 4.1.2-1 Fuel Assembly Stress Analysis Model in the Horizontal Direction

4.1.3. Methodology for the Fuel Assembly Seismic Vertical Response Stress Analysis

For the stress evaluation in the vertical direction of the fuel assembly, all assemblies are assumed to be independent so that the limiting fuel assembly is determined by the relative movement of the upper core plate and lower core support plate at that core location. There are no significant lateral interactive effects among the fuel assemblies and neutron reflectors that are so important in the horizontal seismic analyses.

Consistent with the analyses in the horizontal direction, the stress analyses in the vertical direction for the earthquake and LOCA are performed individually. The procedure is schematically shown in Figure 4.1.3-1 [4-1].

The fuel assembly stress analysis model for the vertical response is shown in Figure 4.1.3-2[4-1]. [ ] In addition, three-dimensional solid elements are used for the detailed stress analyses of the top and bottom nozzles.

The peak vertical load on the fuel assembly, obtained by the reactor internal response analyses, is directly used as input for the stress analyses models for the fuel assembly components, including the top and bottom nozzles. In addition, for the control rod guide thimbles, the vertical load is also used in their buckling evaluation. When the fuel assembly lifts off from the lower core support plate, the relative velocity between the bottom nozzle and the lower core support plate is used as input for the transient analysis with the fuel assembly stress analysis model.

The above stress analyses are individually carried out for the seismic and LOCA events. The stresses in the cladding and the control rod guide thimbles resulting from the SSE analysis are combined with those for LOCA by the SRSS method.

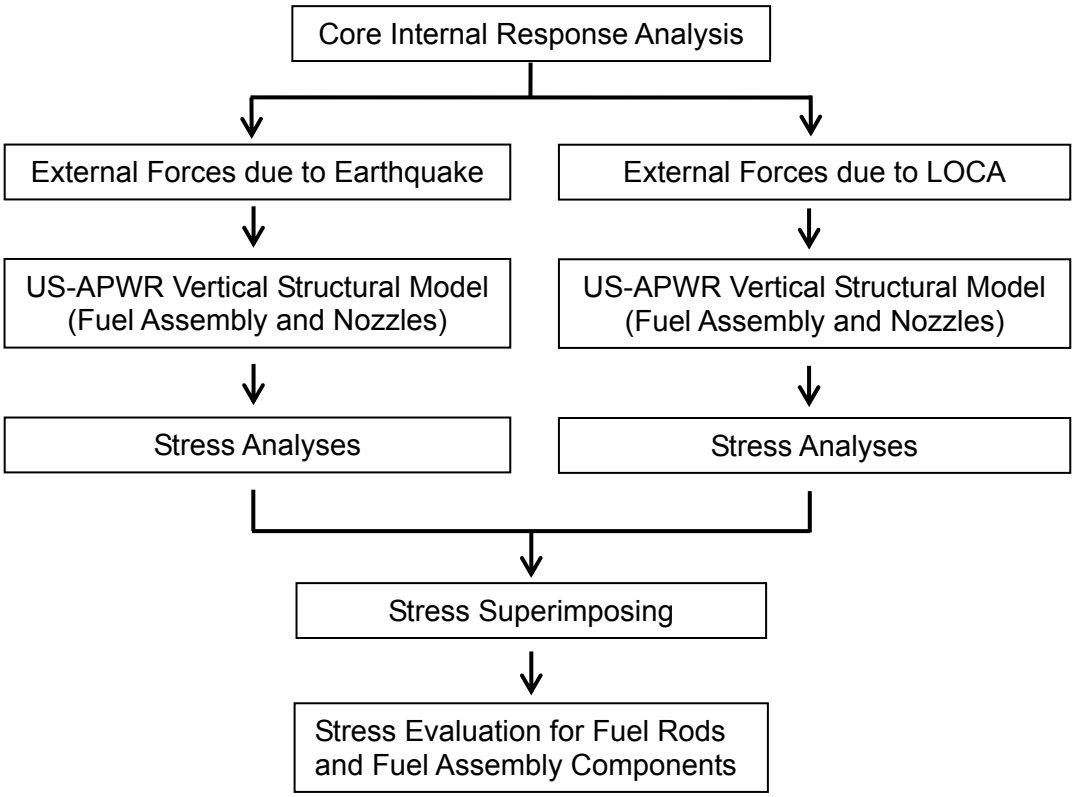

Figure 4.1.3-1 Stress Evaluation for Seismic and LOCA Response in the Vertical Direction

Figure 4.1.3-2 Fuel Assembly Stress Analysis Model for Vertical Response

4.2. Methodology for the Fuel Assembly LOCA Response and Stress Analysis

4.2.1. Methodology for the Fuel Assembly LOCA Horizontal Response Analysis

An acceleration history of the core plates during LOCA is input to the FINDS code for analyzing the fuel assemblies' response. To generate the LOCA acceleration history, an analysis of the reactor coolant system's (RCS) thermal hydraulic transient and an analysis of the reactor vessel and reactor internal's dynamic responses are needed. The RCS thermal hydraulic transient during the blowdown stage of LOCA is analyzed using the MULTIFLEX code, which is described in Section 3.9.1.2.1 of Reference 4-4. The abrupt RCS pressure reduction, due to the pipe break, results in the propagation of a high speed pressure wave in the RCS. The time required for the propagation of the wave around the core barrel creates a pressure differential across the core barrel. This pressure differential results in the vibration of the reactor internals and core barrel. The 3-dimensional dynamic response of the reactor vessel and reactor internals (due to the pressure fluctuations inside the reactor vessel analyzed by the MULTIFLEX code) are analyzed by the ANSYS FEM code. The horizontal time history displacements of the upper and lower core support plates and the vertical loads between the core plates and the fuel assembly nozzles are calculated in this FEM analysis. A flow chart of the analytical procedure is shown in Figure 4.2.1-1.

For the analysis of the horizontal fuel assembly response, the FINDS code is used. The FINDS code was originally developed by MHI for the seismic response analysis of the fuel assemblies array and can also be applied to the analysis for LOCA since the models necessary to determine the fuel assemblies' horizontal response under LOCA conditions is the same as for seismic conditions, as described in Section 3.4.

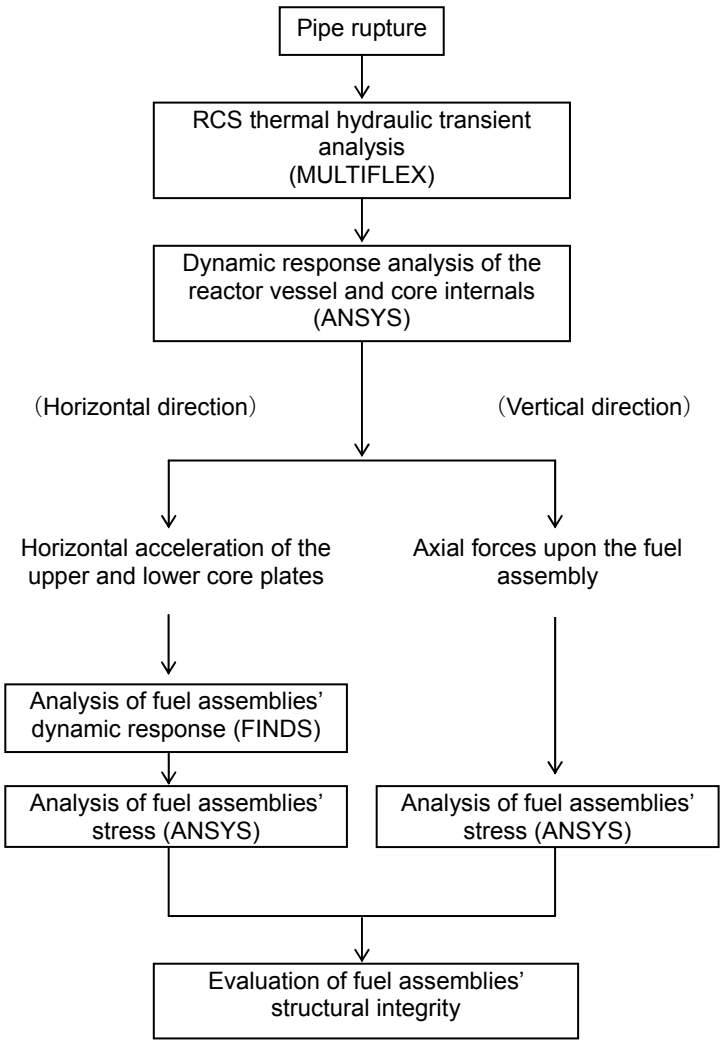

Figure 4.2.1-1 Flow Chart for Determining Fuel Assembly Response and Stresses due to LOCA (RAI Response in Reference 4-5)

4.2.2. Methodology for the Fuel Assembly LOCA Horizontal Response Stress Analysis

Fuel assembly stresses due to the horizontal response during LOCA are evaluated in the same manner as described for seismic conditions in Section 4.1.2.

4.2.3. Methodology for the Fuel Assembly LOCA Vertical Response Stress Analysis

Fuel assembly stresses due to the vertical response during LOCA are evaluated in the same manner as described for seismic conditions in Section 4.1.3.

4.3. Evaluation Results for the Fuel Assembly Response and Strength for Seismic and LOCA Conditions

4.3.1. Results of the Fuel Assembly Horizontal Response Analysis

The horizontal direction response analyses due to the seismic and LOCA by the FINDS code are conducted using the following acceleration wave(4-6) data calculated by the dynamic response analyses of the reactor vessel and reactor internals.

Safe shutdown earthquake (SSE):
- Medium 1 (M1)
- Medium 2 (M2)
- Hard Rock
- Soft

LOCA*:
- CLB 14B 0%
- CLB 14B 102%
- CLB 14B 102%LF
- HLB 10B 102%
- HLB 10B 102%LF

* CLB is cold leg break, HLB is hot leg break,
14B or 10B is the diameter of the pipe which is assumed to break at LOCA.
0% or 102% refers to reactor power.
LF means the vibration force of the loop is considered in the dynamic response analyses of the reactor vessel and reactor internals.

The above four categories of seismic wave data are used to evaluate the capability of the US-APWR standard plant as described in Section 3 of Reference 4-6, and the responses of the upper core plate and lower core support plate are calculated by the dynamic response analyses of the reactor vessel and reactor internals.

For LOCA, the diameters of the nozzles which break at LOCA are determined as 14 inches for cold leg break and as 10 inches for hot leg break, respectively, as described in Section 4 of Reference 4-6. The detailed procedure to calculate the response of the upper core plate and the lower core support plate is described in Section 4.2.1 of this report.

The acceleration time history of the upper core plate and lower core support plate are shown in Figure 4.3.1-1 through 4.3.1-4 for seismic and Figure 4.3.1-5 through 4.3.1-9 for LOCA, respectively. The x direction corresponds to the plant's N-S direction and the z direction corresponds to the plant's E-W direction.

The response analyses are performed for the x and z direction individually, and the responses in the x and z directions are combined by the following equation for both seismic and LOCA, respectively:

$$D\max = \max\left(\sqrt{X_i(t)^2 + Z_j(t)^2}\right)$$

X(t), Z(t): Time history deflection of fuel assembly in x and z direction, respectively
i, j: Fuel assembly number in x and z direction and ranging from 1 to 17, respectively.

The maximum responses obtained in these analyses are shown in Table 4.3.1-1 for SSE and Table 4.3.1-2 for LOCA.

The maximum deflection for SSE is [ ] inch ([ ] mm) in the Medium 1 case. The maximum deflection for LOCA is [ ] inch ([ ] mm) in the CLB 14B 102% case.

The time history responses of the fuel assembly are shown in Figure 4.3.1-10 for seismic and Figure 4.3.1-11 for LOCA, respectively. Figure 4.3.1-10 shows the response for the Medium 1 case as the representative seismic condition and Figure 4.3.1-11 shows the response for the CLB 14B 102% case as the representative LOCA condition.

These deflections are conservative since the analyses were performed on the row with the maximum number of fuel assemblies (17), which enables the highest deflections to occur due to maximizing the available accumulated gaps between the assemblies.

Table 4.3.1-1 Response Analysis Results in Seismic - Horizontal Direction

Wave	Units	SSE M1	SSE M2	SSE Hard Rock	SSE Soft
Maximum displacement	inch (mm)				
Time	s				
Fuel assembly number	-				
Grid number	-				
Maximum impact force*	lbf (N)				
Time	s				
Fuel assembly number **	-				
Grid number	-				
Maximum grid deformation	inch (mm)				

* Buckling force of the grid spacer is [ ] lbf ([ ])N in the FINDS code
** NR refers to Neutron Reflector

Table 4.3.1-2 Response Analysis Results for LOCA - Horizontal Direction (1) CLB 14B Wave

Wave	Units	CLB 14B 0%	CLB 14B 102%LF	CLB 14B 102%
Maximum displacement	inch (mm)			
Time	s			
Fuel assembly number	-			
Grid number	-			
Maximum impact force	lbf (N)			
Time	s			
Fuel assembly number *	-			
Grid number	-			

* NR means the Neutron reflector

Table 4.3.1-2 Response Analysis Results for LOCA - Horizontal Direction (2) HLB 10B Wave

Wave	Units	HLB 10B 102%LF	HLB 10B 102%
Maximum displacement	inch (mm)		
Time	s		
Fuel assembly number	-		
Grid number	-		
Maximum impact force	lbf (N)		
Time	s		
Fuel assembly number	-		
Grid number	-		

Horizontal-Acc.(mm/s^2)

time (sec)

(a) Upper core plate

Horizontal-Acc.(mm/s^2)

time (sec)

(b) Lowe core support plate

Figure 4.3.1-1 Acceleration Time History of the Core Plates for SSE (M1)

Horizontal-Acc.(mm/s^2)

time (sec)

(a) Upper core plate

Horizontal-Acc.(mm/s^2)

time (sec)

(b) Lowe core support plate

Figure 4.3.1-2 Acceleration Time History of the Core Plates for SSE(M2)

Horizontal-Acc.(mm/s^2)

time (sec)

(a) Upper core plate

Horizontal-Acc.(mm/s^2)

time (sec)

(b) Lowe core support plate

Figure 4.3.1-3 Acceleration Time History of the Core Plates for SSE (Hard Rock)

Horizontal-Acc.(mm/s^2)

time (sec)

(a) Upper core plate

Horizontal-Acc.(mm/s^2)

time (sec)

(b) Lowe core support plate

Figure 4.3.1-4 Acceleration Time History of the Core Plates for SSE (Soft)

Horizontal-Acc.(mm/s^2)

time (sec)

(a) Upper core plate

Horizontal-Acc.(mm/s^2)

time (sec)

(b) Lowe core support plate

Figure 4.3.1-5 Acceleration Time History of the Core Plates for LOCA (CLB 14B 0%)

Horizontal-Acc.(mm/s^2)

time (sec)

(a) Upper core plate

Horizontal-Acc.(mm/s^2)

time (sec)

(b) Lowe core support plate

Figure 4.3.1-6 Acceleration Time History of the Core Plates for LOCA (CLB 14B 102%)

Horizontal-Acc.(mm/s^2)

time (sec)

(a) Upper core plate

Horizontal-Acc.(mm/s^2)

time (sec)

(b) Lowe core support plate

Figure 4.3.1-7 Acceleration Time History of the Core Plates for LOCA (CLB 14B 102%LF)

Horizontal−Acc.(mm/s^2)

time (sec)

(a) Upper core plate

Horizontal−Acc.(mm/s^2)

time (sec)

(b) Lowe core support plate

Figure 4.3.1-8 Acceleration Time History of the Core Plates for LOCA (HLB 10B 102%)

Horizontal-Acc.(mm/s^2)

time (sec)

(a) Upper core plate

Horizontal-Acc.(mm/s^2)

time (sec)

(b) Lowe core support plate

Figure 4.3.1-9 Acceleration Time History of the Core Plates for LOCA (HLB 10B 102%LF)

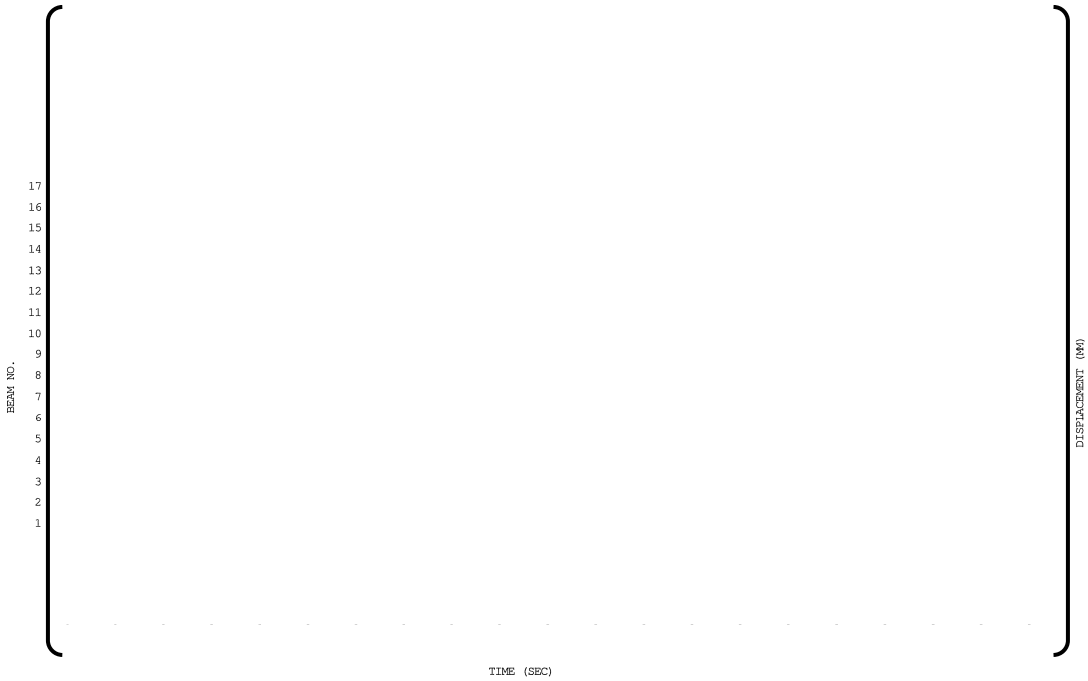

(a) x direction

(b) z direction

Figure 4.3.1-10(1) Fuel Assembly Time History Response (SSE M1) (0 – 10 sec)

(a) x direction

(b) z direction

Figure 4.3.1-10(2) Fuel Assembly Time History Response (SSE M1) (10 – 20 sec)

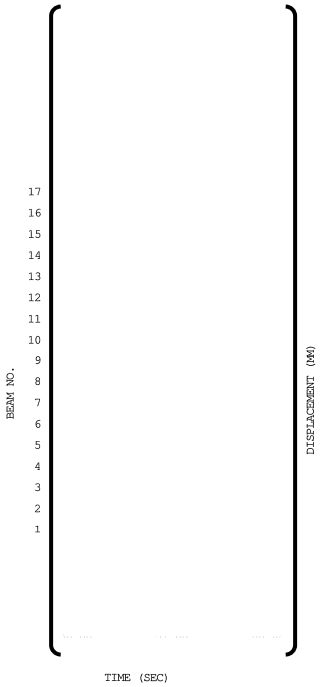

(a) x direction

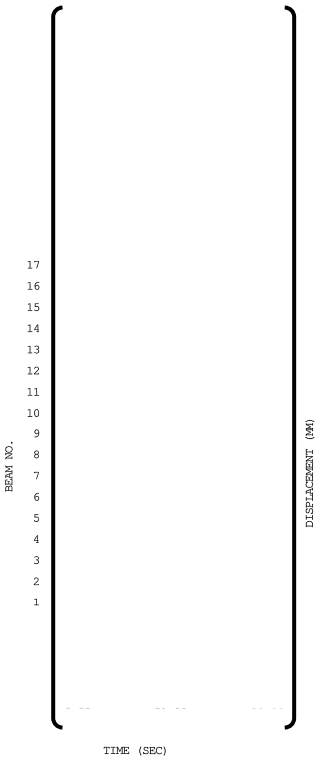

(b) z direction

Figure 4.3.1-10(3) Fuel Assembly Time History Response (SSE M1) (20 – 25 sec)

(a) x direction

(b) z direction

Figure 4.3.1-11 Fuel Assembly Time History Response (CLB 14B 102%)

4.3.2. Stress Evaluation Results of the Fuel Assembly under Safe Shutdown Earthquake and LOCA

The stresses of the fuel assembly due to lateral deflections are calculated using the response to M1 wave shown in Table 4.3.1-1 for SSE and the response to CLB 14B 102% shown in Table 4.3.1-2, respectively, because these waves result in the largest deflection of the fuel assembly for earthquake and LOCA conditions.

The stresses of the fuel assembly due to vertical acceleration are calculated based on the analysis results which are obtained by the reactor internal response analyses to earthquake and LOCA. The relative velocity between the bottom nozzle and the lower core support plate is used as input for the transient analysis model shown in Figure 4.1.3-2 because the fuel assembly lift-off from the lower core support plate occurs in the earthquake and LOCA conditions and then drops on the plate.

The maximum stress obtained by combining the stresses for the earthquake and LOCA by the SRSS method is shown in Table 4.3.2-2.

As shown in Table 4.3.2-2, the resulting stress is lower than the acceptance limit and it is therefore confirmed that each component has the required strength. Grid deformation occurs in the earthquake condition and this deformation causes control rod guide thimble and fuel cladding distortion. Therefore the stress caused by the grid deformation is calculated and superimposed on the stress due to normal operation and fuel assembly deflection (from the horizontal direction) by the SRSS method.

The Medium 1 wave and the CLB 14B 102% wave are also conservatively used as the representative earthquake and LOCA conditions respectively for the irradiated fuel assembly in Appendix A of this report.

Table 4.3.2-1 Peak Vertical Load for Fuel Assembly under Safe Shutdown Earthquake (M1) and LOCA (CLB 14B 102%)

Item	Units	SSE M1	CLB 14B 102%
Holddown Spring Reaction Force	lbf (N)		
Drop Velocity*	inch/s (mm/s)		

* Drop velocity means the relative velocity between the bottom nozzle and the lower core support plate.

Table 4.3.2-2 Stress Analysis Results for the Fuel Assembly under Safe Shutdown Earthquake (M1) and LOCA (CLB 14B 102%)

(a) Control rod guide thimble

Unit: ksi (MPa)

Stress Category	NO	SSE & LOCA	NO + SSE & LOCA	Acceptance limit at [ ] deg.F
Primary Membrane Stress				
Primary Membrane Stress + Primary Bending Stress				

* Stress due to vertical load

** Stress due to vertical load and horizontal displacement and distortion caused by the grid deformation

(b) Top nozzle

Unit: ksi (MPa)

Stress Category	NO	SSE & LOCA	NO + SSE & LOCA	Acceptance limit at [ ] deg.F
Primary Membrane Stress + Primary Bending Stress				

* Stress due to the vertical load

(c) Bottom nozzle

Unit: ksi (MPa)

Stress Category	NO	SSE & LOCA	NO + SSE & LOCA	Acceptance limit at [ ] deg.F
Primary Membrane Stress + Primary Bending Stress				

* Stress due to the vertical load

(d) Grid spacer

Unit: inch (mm)

Maximum deformation	Acceptance limit
	No excessive deformation shall occur due to load during an accident.

(e) Buckling of control rod guide thimble

Unit: lbf (N)

Maximum force	Acceptance limit

Table 4.3.2-2(Continued) Stress Analysis Results for the Fuel Assembly under Safe Shutdown Earthquake (M1) and LOCA (CLB 14B 102%)

(f) Fuel cladding

Unit: ksi (MPa)

Stress Category	NO +SSE & LOCA	Acceptance limit*
Primary Membrane Stress		
Primary Membrane Stress + Primary Bending Stress + Local Membrane Stress		

* Acceptance limit at the fuel cladding temperature

4.4. References

(4-1) “Mitsubishi Fuel Design Criteria and Methodology”, MUAP-07008-P (Proprietary) and MUAP-07008-NP (Non-Proprietary), May 2007

(4-2) “FINDS: Mitsubishi PWR Fuel Assemblies Seismic Analysis Code”, MUAP-07034-P (Proprietary) and MUAP-07034-NP (Non-Proprietary), March 2008

(4-3) MHI's Responses to the NRC's Requests for Additional Information on Topical Report MUAP-07034-P “FINDS: Mitsubishi PWR Fuel Assemblies Seismic Analysis Code", UAP-HF-08139-P (Proprietary) and MUAP-08139-NP (Non-Proprietary), August 2008

(4-4) ”Design Control Document for the US-APWR”, MUAP-DC003 Revision 1, August 2008

(4-5) MHI’s Responses to the NRC’s Requests for Additional Information on Topical Report MUAP-07034-P(0) “FINDS: Mitsubishi PWR Fuel Assemblies Seismic Analysis Code”, UAP-HF-08309-P(Proprietary) and UAP-HF-08309-NP (Non-Proprietary), December 2008

(4-6) “Summary of Seismic and Accident Load Conditions for Primary Components and Piping”, MUAP-09002-P (Proprietary) and MUAP-09002-NP (Non-Proprietary), January 2009

5.0 STRESS ANALYSIS OF THE ROD CLUSTER CONTROL ASSEMBLY FOR SEISMIC AND LOCA EVENTS

5.1. Stress Evaluation Methodology for Rod Cluster Control Assembly

5.1.1. Stress Analysis Model for Rod Cluster Control Assembly for Seismic and LOCA

During normal operating conditions, the RCCA drive rod is engaged with the CRDM near its middle and with the RCCA spider hub at the bottom. The RCCA is supported laterally over short span lengths by the guide plates of control rod guide tube.

In the RCCA scram state, the RCCA drops into the fuel assembly. In seismic or LOCA events, the fuel assembly deflects laterally and the control rods deform laterally as well during insertion. The flow chart, shown in Figure 5.1.1-1, is used to determine the control rod stresses associated with the lateral deformations generated in both seismic and LOCA events.

The stresses of the control rod are evaluated at three representative axial positions 1) fully withdrawn from the fuel assembly, 2) half inserted and 3) fully inserted into the fuel assembly, as shown in Figure 5.1.1-2. The resulting stress of the control rod when fully withdrawn is very small due to the reason described in Section 5.2 for seismic and 5.3 for LOCA and is negligible compared with the acceptance limit. In the half inserted and fully inserted positions, the stresses of the control rod are evaluated by an FEM model considering the maximum deformations of the fuel assembly in the seismic or LOCA event. The stress due to LOCA is combined with the stress due to an SSE using the SRSS method. The stresses of the cladding and the reduced diameter portion of the control rod top end plug are evaluated in the analysis.

The FEM analysis model for the RCCA consists of several elastic beams which represent each component of the RCCA, as shown in Figure 5.1.1-3.

The stresses due to the vertical response of the RCCA in the seismic and LOCA events are calculated using the same model as shown in Figure 5.1.1-3, considering the maximum vertical acceleration of the CRDM which is obtained by the dynamic response analysis of the reactor vessel and reactor internals. The flow chart for this stress evaluation is shown in Figure 5.1.1-4. The stress due to LOCA is combined with the stress due to an SSE using the SRSS method.

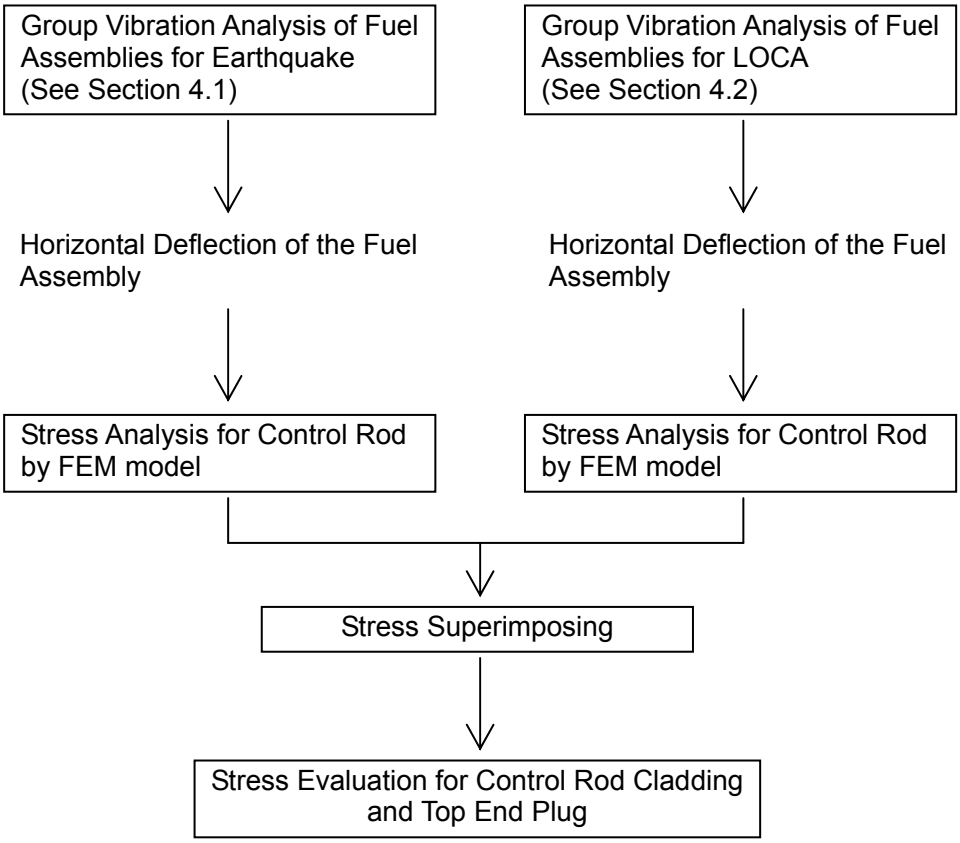

Figure 5.1.1-1 Stress Evaluation for the Control Rod Assembly due to Fuel Assembly Horizontal Deflection during a Seismic and LOCA Event

Figure 5.1.1-2 Axial Positions of RCCA for Stress Evaluation

Actual RCCA Beam Model for RCCA

Figure 5.1.1-3 Analysis Model for RCCA

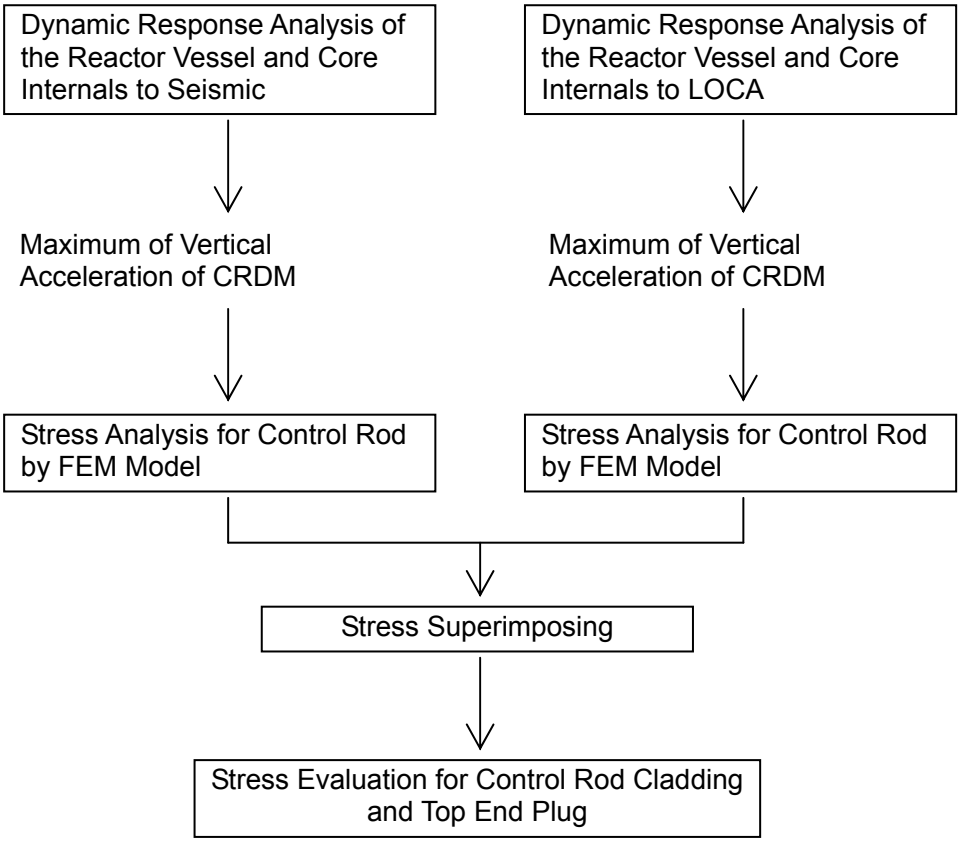

Figure 5.1.1-4 Stress Evaluation for the Control Rod Assembly due to Vertical Acceleration during a Seismic and LOCA event

5.1.2. Stress Evaluation Method for the Rod Cluster Control Assembly

The stresses due to the horizontal deflection and vertical acceleration are combined with the SRSS method. In addition to the above stresses, the effect of the CRDM stepping loads or the scram impact load is taken into account when half inserted and fully inserted, respectively. All of these stresses are added each other.

The stress due to the pressure differential (system pressure versus control rod internal pressure) is also evaluated and added to the stresses calculated above.

The stress categories used in evaluating the integrity of the control rod assembly are summarized in Table 5.1.2-1.

Table 5.1.2-1 Stress Categories

Loading Conditions	Stress Category	Classification
Lateral deformation due to deflection of fuel assembly during seismic and LOCA	Primary Bending Stress	Pb
Vertical acceleration during seismic and LOCA	Primary Membrane Stress	Pm
Stepping Load of CRDM or RCCA Scram Impact Load	Primary Membrane Stress	Pm
Inner-outer differential pressure	Primary Membrane Stress	Pm

5.2. Stress Evaluation of Rod Cluster Control Assembly under Safe Shutdown Earthquake and LOCA

5.2.1. Stress Analysis of Rod Cluster Control Assembly due to Safe Shutdown Earthquake

As described in Section 2.2 of the report, the stresses of the cladding and the reduced diameter portion of the top end plug of the control rod are evaluated.

Of the three representative axial positions of the RCCA relative to the fuel assembly, the resulting stress when the RCCA is fully withdrawn is very small because the lateral deformation of the control rod guide tube during seismic events is very small and the control rod is supported by the guide plates over short span lengths, of about [ ] inch ([ ] mm) or less. Therefore, the deflection of the control rod is small and the resulting stresses of the control rod at the fully withdrawn position during SSE conditions are negligible compared with the acceptance limit. On the other hand, in the half inserted and fully inserted axial positions, the stress of the control rod is evaluated because it is affected by the deflection of the fuel assembly. The maximum deflection of the fuel assembly for an SSE is obtained from the response analysis described in Section 4.3.1. The analysis result for the M1 wave is used for the stress analysis of the control rod because the deflection of the fuel assembly is larger compared with the other waves and therefore results in a conservative evaluation. The maximum lateral displacements of each fuel assembly's grid spacers determine the shape of the control rod used in the model shown in Figure 5.1.1-3 to estimate the stress of the control rod.

The calculated stress of the control rod due to lateral deformation is shown in Table 5.2.1-1.

The stress due to the vertical acceleration is calculated considering the maximum acceleration obtained from the dynamic analysis of the reactor vessel and reactor internals of [ ] inch/s^2 ([ ] mm/s^2). Applying the acceleration to the model shown in Figure 5.1.1-3 vertically, the stresses of the limiting components are evaluated.

The calculated stress of the control rod assembly due to vertical acceleration is also shown in Table 5.2.1-1.

Table 5.2.1-1 Stresses of Control Rod due to Safe Shutdown Earthquake

Unit: ksi (MPa)

	Stress category	Cladding of control rod	Top end plug of control rod (Reduced diameter portion)
Half inserted	Primary Membrane Stress	[ ]	
	Primary Membrane Stress + Primary Bending Stress		
Fully inserted	Primary Membrane Stress		
	Primary Membrane Stress + Primary Bending Stress		

* Stress due to vertical acceleration
** Stress due to vertical acceleration and lateral deflection

5.2.2. Stress Analysis of Rod Cluster Control Assembly for LOCA Events

The stresses in the control rod cladding and the reduced diameter portion of the top end plug due to a LOCA event is calculated in the same manner as for a seismic event.

Of the three representative axial positions of the RCCA relative to the fuel assembly, the resulting stress when the RCCA is fully withdrawn is very small because the lateral deformation of the control rod guide tube during LOCA is very small and the control rod is supported by the guide plates over short span lengths, as described in Section 5.2.1. Therefore, the resulting stresses of the control rod when fully withdrawn during LOCA conditions are negligible compared with the acceptance limit. On the other hand, in the half inserted and fully inserted axial positions, the stress of the control rod is evaluated considering the deformation of the fuel assembly during a LOCA as described in Section 4.3.1. The analysis result for the CLB 14B 102% wave is used for the stress analysis of the control rod because the deflection of the fuel assembly is larger compared with the other waves and results in a conservative evaluation. The displacements at each grid spacer, obtained from the fuel assembly's response analysis, are used to define the deflected control rod shape input to the model shown in Figure 5.1.1-3.

The calculated stress of the control rod due to lateral deformation is shown in Table 5.2.2-1.

The stress due to the vertical acceleration is calculated considering the acceleration of [ ] inch/s^2 ([ ] mm/s^2), which is the maximum acceleration obtained from the dynamic analysis of the reactor vessel and reactor internals. The stresses of the limiting components are evaluated by applying this acceleration to the model shown in Figure 5.1.1-3.

The calculated stresses due to the lateral deformation and vertical acceleration during LOCA are shown in Table 5.2.2-1.

Table 5.2.2-1 Stresses of Control Rod in LOCA

Unit: ksi (MPa)

	Stress category	Cladding of control rod	Top end plug of control rod (Reduced diameter portion)
Half inserted	Primary Membrane Stress	[	]
	Primary Membrane Stress + Primary Bending Stress		
Fully inserted	Primary Membrane Stress		
	Primary Membrane Stress + Primary Bending Stress		

* Stress due to vertical acceleration
** Stress due to vertical acceleration and lateral deflection

5.2.3. Stress Evaluation Results of Rod Cluster Control Assembly for Combined Safe Shutdown Earthquake and LOCA Events

In addition to the stress due to SSE and LOCA, the effect of the CRDM stepping loads described in Table 5.1-2 of Reference 5-1 is considered in the evaluation for a half withdrawn RCCA. For a fully inserted RCCA, the RCCA scram impact load of [ ] lbf ([ ] N) is used as described in Section 4.1.2.2.1 of Reference 5-1.

Also, the effect of differential pressure (system pressure versus control rod internal pressure) is taken into account. The maximum system pressure of [ ] ksi ([ ] MPa) is used and an internal pressure of [ ] psi ([ ] MPa) at cold condition is used for conservatism.

The evaluation results are summarized in Table 5.2.3-1 to confirm the RCCA integrity in the combined SSE and LOCA events.

Table 5.2.3-1 Stress Evaluation Results for Control Rod

(a) Cladding of control rod

Unit: ksi (MPa)

	Stress Category	Stress	Acceptance Limit @ [ ] * deg.F(5-1)
Half inserted	Primary Membrane Stress	[ ]	
	Primary Membrane Stress +Primary Bending Stress		
Fully inserted	Primary Membrane Stress		
	Primary Membrane Stress +Primary Bending Stress		

* Obtained from thermal analysis performed for the control rod

(b) Top end plug of control rod (reduced diameter portion)

Unit: ksi (MPa)

	Stress Category	Stress	Acceptance Limit @ [ ] ** deg.F(5-1)
Half inserted	Primary Membrane Stress	[ ]	
	Primary Membrane Stress +Primary Bending Stress		
Fully inserted	Primary Membrane Stress		
	Primary Membrane Stress +Primary Bending Stress		

** Outlet temperature of the core

5.3. References

(5-1) "US-APWR Fuel System Design Evaluation", MUAP-07016-P (Proprietary) and MUAP-07016-NP (Non-Proprietary), February 2008

6.0 CONCLUTION

This report describes the functional requirements and acceptance criteria of the US-APWR fuel system, namely the fuel assembly and the rod cluster control assembly, during Safe Shutdown Earthquake (SSE) and LOCA. Also, the evaluation results for dynamic response and for the integrity of the fuel system are included in the report to confirm that the required functions are maintained during these events.

The effects of irradiation on the fuel system response under SSE and LOCA were also discussed in the report to show that the integrity of the fuel system is maintained under irradiated conditions.

Appendix A

EVALUATION RESULTS FOR AN IRRADIATED FUEL SYSTEM UNDER SEISMIC AND LOCA CONDITIONS

March 2009

Table of Contents

List of Tables

List of Figures

A.1.0 INTRODUCTION

The spring force of the grid spacer decreases during irradiation, primarily due to irradiation induced stress relaxation. The reduced grid spring force can affect the fuel assembly's dynamic behavior during an earthquake or LOCA. In this Appendix, the effect of the relaxation of the grid spacer spring force on the fuel assembly's vibration behavior is investigated analytically.

Also, the grid spacer's behavior, as a result of repeated impacts, is characterized using grid impact test results with the as-built and relaxed grid spring force.

Based on these results, a seismic and LOCA response analyses for a fuel assembly with relaxed grid spring force is performed and the fuel assembly's integrity is evaluated.

The effect of the reduced ductility of the grid spacer material (due to irradiation hardening) on the grid spacer's crush strength and deformation behavior is also described in this Appendix.

A.2.0 EFFECT OF IRRADIATION ON FUEL ASSSEMBLY VIBRATION CHARACTERISTICS

A.2.1. Analytical Model and Method

According to Reference A-5, by end of life the grid spacer grid springs are expected to relax to [ ] percent or [ ] percent of their initial values. The effect of reduced grid spacer spring force on the vibration characteristics of the fuel assembly, such as the amplitude dependent frequency and the amplitude dependent damping is evaluated using the ANSYS FEM code. The analysis model is shown in Figure A.2.1-1.

The stress analysis model shown in Figure 4.1.2-1 of this report, which is for static analysis, is also used for predicting the irradiation effects on the fuel assembly's dynamic properties. [ ]

The detailed explanation of the model is described in Appendix A of Reference A-1.

Figure A.2.1-1 Fuel Assembly Stress Analysis Model in the Horizontal Direction

A.2.2. Analysis Results

The effect of the grid spring relaxation is evaluated using the model described in Section A.2.1 of this report and in Reference A-2.

To study the fuel assembly dynamic response with this model, the centermost middle grid spacer is laterally displaced, with all other fuel assembly model boundary conditions the same as used in a fuel assembly free vibration test. The centermost grid is released quickly and the time history displacement at each grid spacer position is calculated.

For the analysis model with relaxed grid spring force, the forces are determined to be [ ] percent of the initial value for the top grid spacer, [ ] percent for the middle grid spacers and [ ] percent for the bottom grid spacer, to simulate an irradiated fuel assembly at a burn-up of 60 GWd/t.

Both the as-built spring force and relaxed grid spring force models have the top and bottom ends restrained when the centermost middle grid spacer is initially displaced, and then quickly released. The maximum initial displacements were [ ] inch ([ ] mm) for the as-built spring force model and [ ] inch ([ ] mm) for the relaxed grid spring force model. The larger initial displacement has been given to the relaxed spring force model because the larger deflection has been expected in the seismic analysis described in Section A.4.0 of the report. Based on the time history displacement data, the amplitude dependence of frequency and damping of the fuel assembly with the relaxed spring force are calculated as shown in Figure A.2.2-1. The analyses are conducted at cold in air condition.

The amplitude dependence of the frequency and damping factor is due to the contact and slippage mechanism between the fuel rods and grid spacers. As the vibration amplitude increases the natural frequency decreases and, conversely, the damping factor increases due to slippage at the contact points.

[ ]

The vibration characteristics for the fuel assembly with relaxed grid spring force, used in the FINDS analysis, is developed based on the ANSYS analysis results. The amplitude dependence of the natural frequency at reactor conditions is determined considering the effect of the coolant as the added mass as described in 4.1.1.2.1 of this report. The amplitude dependence of the damping is determined based on the ANSYS analysis results for cold in air condition for conservatism.

Frequency (Hz)

Peak-average amplitude (mm)

(a) Natural frequency

Damping factor (-)

Peak-average amplitude (mm)

(b) Damping factor

Figure A.2.2-1 Amplitude Dependence of the 14ft Fuel Assembly's Frequency and Damping using ANSYS FEM Analysis (Cold in Air Condition)

A.3.0 EFFECT OF IRRADIATION ON GRID SPACER CRUSH BEHAVIOR

A.3.1. Effect of Grid Spacer's Spring Relaxation

A Zr-4 grid spacer's spring force typically relaxes significantly during irradiation, which may have an effect on the grid spacer's crush behavior. To investigate the influence of this grid spring force relaxation, grid spacer impact tests were performed with grid spacers whose spring force was relaxed in a furnace to simulate end of life conditions.

A.3.1.1. Impact Test of Grid Spacers with Relaxed Spring Force

(1) Tested Grid Spacers

The following Z3 type of Zircaloy-4 grid spacers, which are intended to be used in the US-APWR fuel assembly, were tested.

- Grid spacers with as-built spring force (As-built grid spacers) ---- 6 Grid Spacers
- Grid spacers with relaxed spring force (Relaxed grid spacers) ---- 8 Grid Spacers

The process of reducing the spring force begins with inserting short solid stainless steel rods, of a larger diameter than the fuel rod cladding, into all of the fuel rod cells. To relax the spring force, the grid spacers are then placed in a furnace at [ ] deg. F ([ ] deg. C) for [ ] hours. The permanent cell size increase occurs due to yielding of the Zr-4 material and thermal creep at the elevated temperature. The temperature, time in the furnace and the diameter of the stainless steel rod were empirically determined to enlarge the cell size so that the spring force after the relaxation process corresponded to approximately 5% of the as-built spring force. Short sections of 17x17 fuel rod clad replaced the stainless steel rods when the grid spacers were used in the impact tests.

(2) Test Procedure

The impact tests for the grid spacers were performed by a pendulum impact test apparatus as shown in Figure A.3.1.1-1. A furnace, not shown in the Figure, is placed around the grid spacer to heat it to the test temperature (not shown in the figure). To perform the impact test the furnace is quickly removed and replaced with the weight. The weight at the end of the pendulum arm impacts with the grid spacer that is attached to a rigid wall. Considering reactor operating temperatures the grid spacer is heated up to [ ] deg. F ([ ] deg. C). Grid temperatures during heat-up and at impact are monitored by thermocouples.

A load cell on the rigid wall and an accelerometer on the weight are used to determine impact force and load-displacement characteristics. An angular transducer at the top end of the pendulum arm senses the release angle and rebound angle needed to calculate the coefficient of restitution. The swinging weight is prevented from re-impacting the grid spacer after achieving its maximum rebound angle.

The impact test is repeatedly performed at increasing release angles and continues to and beyond the buckling load of the grid spacer.

(3) Data reduction

Physical data obtained by the test are reduced as follows.

<Weight velocity at the impact>

Before the grid impact test is performed, a free vibration test is conducted to obtain the relationship between pendulum arm release angle and the velocity of the weight at the moment of grid impact. The weight's velocity dependence on release angle is calculated by following equation.

$$V(\theta_0)=2PL_0\mathrm{Sin}(\theta_0/2)$$

where

$V(\theta_0)$: Weight's velocity (m/sec) at grid impact when release angle is θ_0.
θ_0 : Release angle (Degree)
P : P is obtained by following equation as a function of a quarter cycle of the pendulum and the first order of the elliptic integral.

$$P=\frac{1}{T}K\left(k^2\right)$$

where

T : Quarter cycle of the pendulum (sec), T is determined by the pendulum arm's displacement history which is measured by the angular transducer in the free vibration tests of the pendulum.
$K(k^2)$: The first order of the elliptic integral for $k= \sin(\theta_0/2)$

P is calculated in Table A.3.1.1-1 and the averaged value of ( ) is used in the velocity calculation.
L_0 : Pendulum arm length, 1 (m)

<Buckling Load>

Since the impact force tends to be lower after buckling, the buckling force is defined as the highest impact force measured at the step before the impact force begins to decrease.

<Dynamic Stiffness>

Using the method of least squares, the slope "a" (F/V) is obtained for a linear relationship between the impact velocity of the weight and the impact force before buckling.

In addition, the following relationship between the impact velocity of the weight and the impact force before buckling is used.

$$F=\sqrt{M_{eq}K}V$$

where

K : Dynamic stiffness of the grid spacer
M_{eq} : Equivalent mass of the weight
F : Impact force measured by load cell sensor
V : Impact velocity of the weight

The dynamic stiffness of the grid spacer is calculated by using the equation "a" = $\sqrt{M_{eq}K}$ and solving for K.

< Coefficient of Restitution>

The coefficient of restitution is defined as ratio of the rebound angle to the release angle of the pendulum arm. The angle is measured by the angular transducer.

(4) Test results

Figure A.3.1.1-2 and Figure A.3.1.1-3 show the relationship between impact force and impact velocity for the as-built and the relaxed grid spacers, respectively. In addition, Figure A.3.1.1-4 and Figure A.3.1.1-5 illustrate the relationship between the coefficient of restitution and impact velocity of both types of grid spacers, respectively.

Although it can be seen in Figure A.3.1.1-2 that the impact force of the as-built grid spacer is increasing again after the 20 inch/sec velocity, the buckling force is defined as the impact force at around 17 inch/sec because the coefficient of restitution for the as-built grid spacers is predominantly decreasing after about 17 inch/sec. On the other hand, the trend of the buckling force of the relaxed grid spacers continually decrease after buckling at around 17 inch/sec, as seen in Figure A.3.1.1-3.

The buckling force for both conditions of the grid spacers is summarized in Table A.3.1.1-2 and Table A.3.1.1-3. Based on the comparison of the average buckling force, the decrease in the buckling force due to the relaxed spring force is calculated to be [ ] %.

Using the test data for the buckling forces of the grid spacers, the 95% confidence values of the true mean are calculated, consistent with Reference A-3, for grid spacers with as-built spring force and relaxed spring force. The calculated 95% confidence values are shown in Table A.3.1.1-2 for the grid spacer with as-built spring force, and in Table A.3.1.1-3 for the grid spacer with relaxed spring force. Based on the comparison of the lower bound buckling force, the decrease in the buckling force due to the relaxed spring force is calculated to be [ ] %.

Table A.3.1.1-1 Free Vibration Pendulum Test Results

Release Angle :θ_0 (degree)	Sin(θ_0/2) : k	k^2	K(k^2)	1/4 Cycle :T (sec)	P=K(k^2)/T (1/sec)
2					
4					
6					
8					
10					
12					
14					
16					
18					
20					

Table A.3.1.1-2 Buckling Force of the As-built Grid Spacers

Grid Spacer No.	Buckling Force		Dynamic Stiffness	
	(lbf)	(kN)	(lbf/inch)	(kN/mm)
As-Built_1				
As-Built_2				
As-Built_3				
As-Built_4				
As-Built_5				
As-Built_6				
Ave.				
Std.				
95% confidence*				

Table A.3.1.1-3 Buckling Force of the Relaxed Grid Spacers

Grid Spacer No.	Buckling Force		Dynamic Stiffness	
	(lbf)	(kN)	(lbf/inch)	(kN/mm)
Relaxed_1				
Relaxed_2				
Relaxed_3				
Relaxed_4				
Relaxed_5				
Relaxed_6				
Relaxed_7				
Relaxed_8				
Ave.				
Std.				
95% confidence*				

* 95% confidence level based on the true mean of the test results

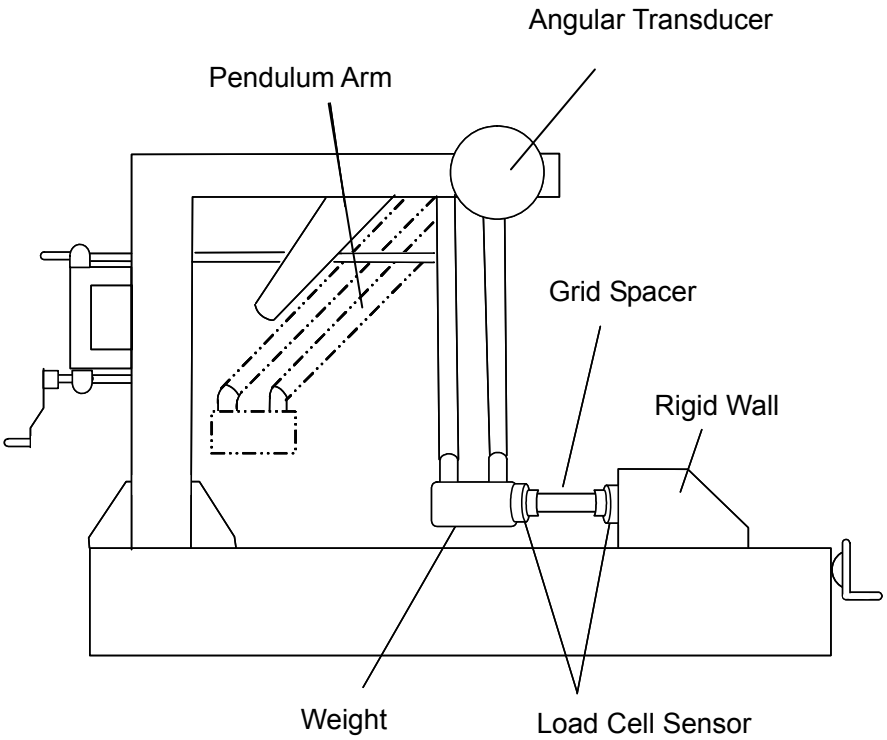

Figure A.3.1.1-1 Grid Spacer and Pendulum Type Impact Test

Impact Force (lbf)

Impact Velocity of the Weight (inch/sec)

Figure A.3.1.1-2 Impact Force versus Impact Velocity (As-built Grid Spacers)

Impact Force (lbf)

Impact Velocity of the Weight (inch/sec)

Figure A.3.1.1-3 Impact Force versus Impact Velocity (Relaxed Grid Spacers)

Restitution Coefficient (-)

Impact Velocity of the Weight (inch/sec)

Figure A.3.1.1-4 Coefficient of Restitution vs Impact Velocity (As-built Grid Spacers)

Restitution Coefficient (-)

Impact Velocity of the Weight (inch/sec)

Figure A.3.1.1-5 Coefficient of Restitution vs Impact Velocity (Relaxed Grid Spacers)

A.3.1.2. In-elastic Impact Model of the Grid Spacer with Relaxed Spring Force

As part of the grid impact test series, two each of the as-built and the relaxed grid spacers were used to perform a deformation progression test in order to generate the in-elastic models of the grid spacers in both conditions for use in the FINDS code.

As described in Subsection 3.7.3 in Reference A-4, the deformation progression test is used to obtain the characteristics of the grid spacers energy storage capacity in the post-buckling phase. Basically the grid impact test is sequentially continued with the same or increased release angles until the grid spacer shows significant plastic deformation. During the test series, the plastic deformation is defined by the reduction in the grid spacer's envelope as measured by a vernier caliper. As-Built_5, As-Built_6, Relaxed_7 and Relaxed_8 were used in the deformation progression test. The test sequence is shown in Table A.3.1.2-1. The tests were also performed with the temperature of the grid spacer at [ ] deg. F ([ ] deg. C).

Impact force, plastic deformation and the coefficient of restitution obtained by the deformation progression tests are used to adjust the grid spacer's in-elastic models used in the FINDS code, as described in Subsection 4.2 of Reference A-4. A comparison between analytical and experimental results for the as-built grid spacers are shown in the following figures.

Figure A.3.1.2-1(a) Impact Force (As-Built_5)
Figure A.3.1.2-1(b) Impact Force (As-Built_6)
Figure A.3.1.2-2(a) Plastic Deformation (As-Built_5)
Figure A.3.1.2-2(b) Plastic Deformation (As-Built_6)
Figure A.3.1.2-3(a) Coefficient of Restitution (As-Built_5)
Figure A.3.1.2-3(b) Coefficient of Restitution (As-Built_6)

Although the buckling of the as-built grid spacers is regarded as having occurred in test sequence No.3, the increase in impact force until test sequence No.9 or No.10 in Figure A.3.1.2-1(a) and (b) is simulated by the FINDS code model.

Plastic deformation of the as-built grid spacer is conservatively modeled as shown in the Figure A.3.1.2-2(a) and (b).

The same comparisons as in Figure A.3.1.2-1 thorough Figure A.3.1.2-3, but for the relaxed grid spacers, are shown in Figure A.3.1.2-4 thorough Figure A.3.1.2-6. The impact force for the relaxed grid spacers is well simulated by the empirically adjusted model, as shown in Figure A.3.1.2-4(a) and (b). There is a little difference in the plastic deformation between the two tested grid spacers, however, and the FINDS code conservatively models the plastic deformation, as seen in Figure A.3.1.2-5(a) and (b).

Since the as-built and the relaxed grid spacer models developed here are for full-sized grid spacers, the models are adapted to the two half-sized grid spacers used in the FINDS code according to the procedure described in Subsection 4.2.2 in Reference A-4.

Table A.3.1.2-1 Test Sequence for Deformation Progression (before buckling included)

Test Sequence (No.)	Pendulum Release Angle (Degree)	
	Grid spacers As-Built_5 and As-Built_6	Grid spacers Relaxed_7 and Relaxed_8
1		
2		
3		
4		
5		
6		
7		
8		
9		
10		
11		
12		
13		
14		
15		
16		
17		
18		
19		

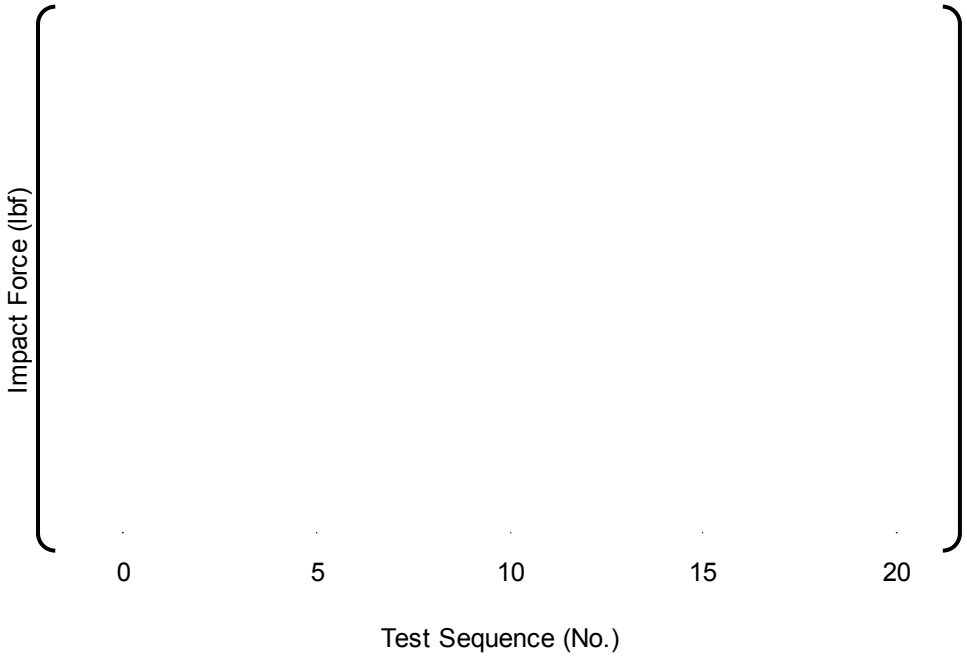

Figure A.3.1.2-1(a) Impact Force (As-Built_5)

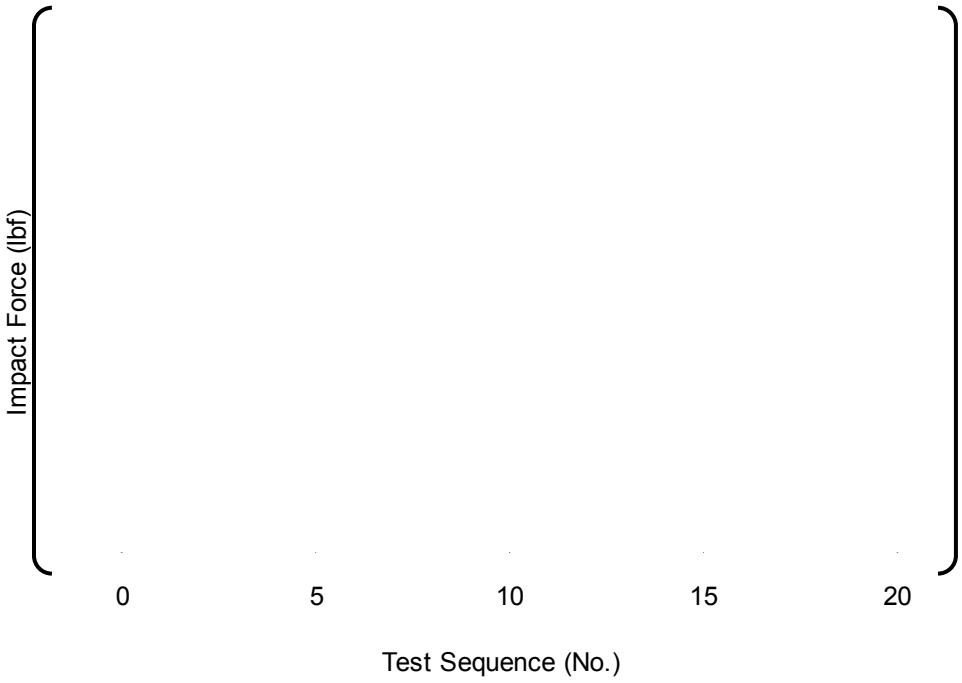

Figure A.3.1.2-1(b) Impact Force (As-Built_6)

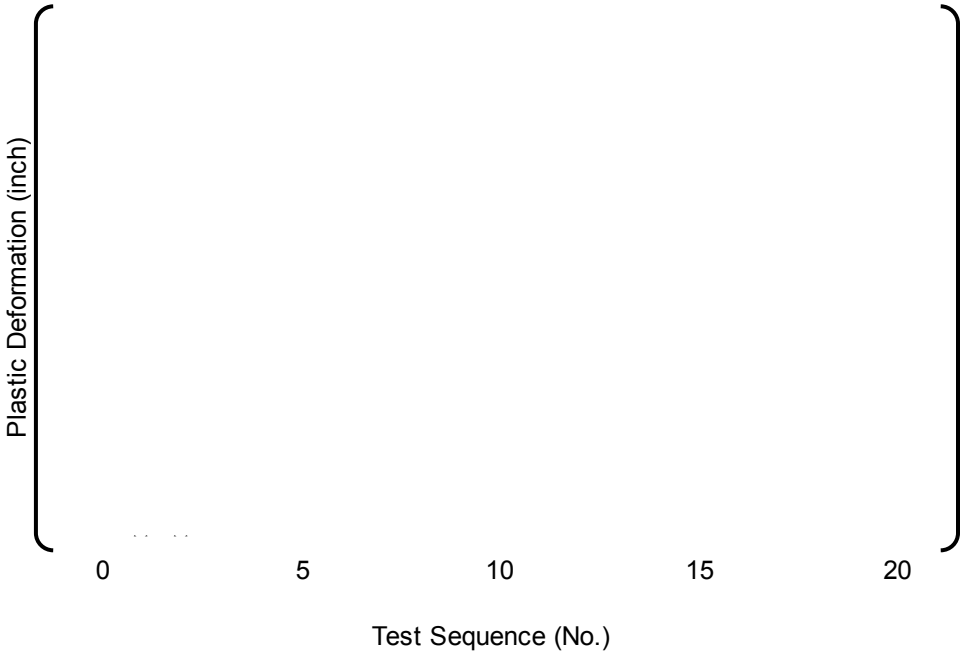

Figure A.3.1.2-2(a) Plastic Deformation (As-Built_5)

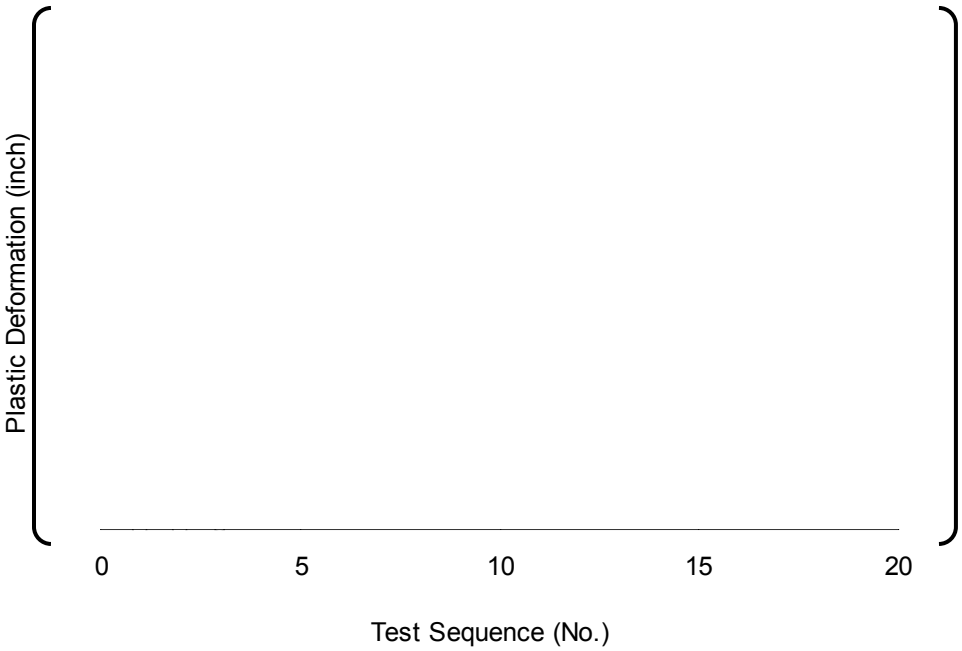

Figure A.3.1.2-2(b) Plastic Deformation (As-Built_6)

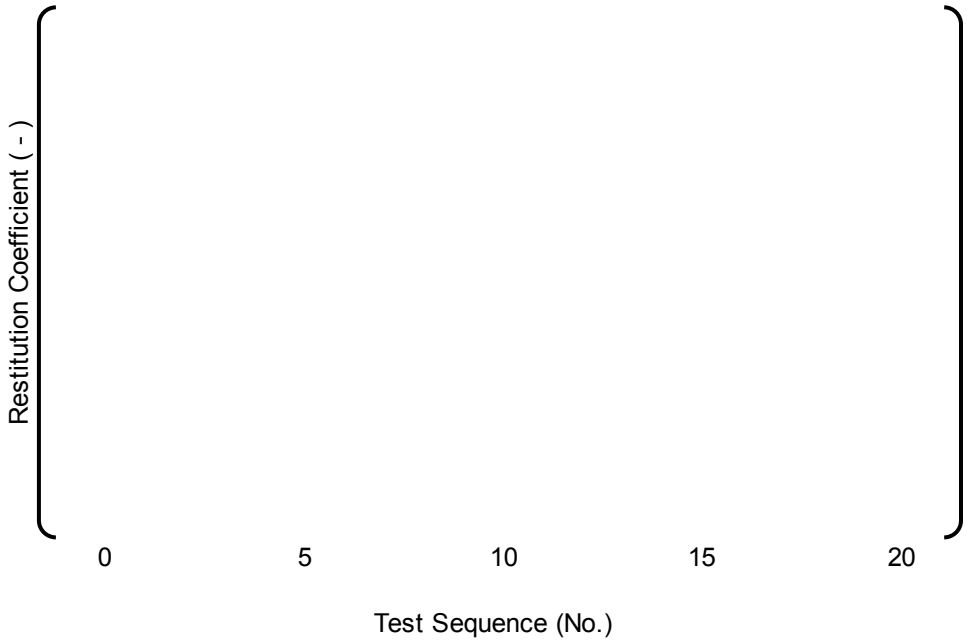

Figure A.3.1.2-3(a) Coefficient of Restitution (As-Built_5)

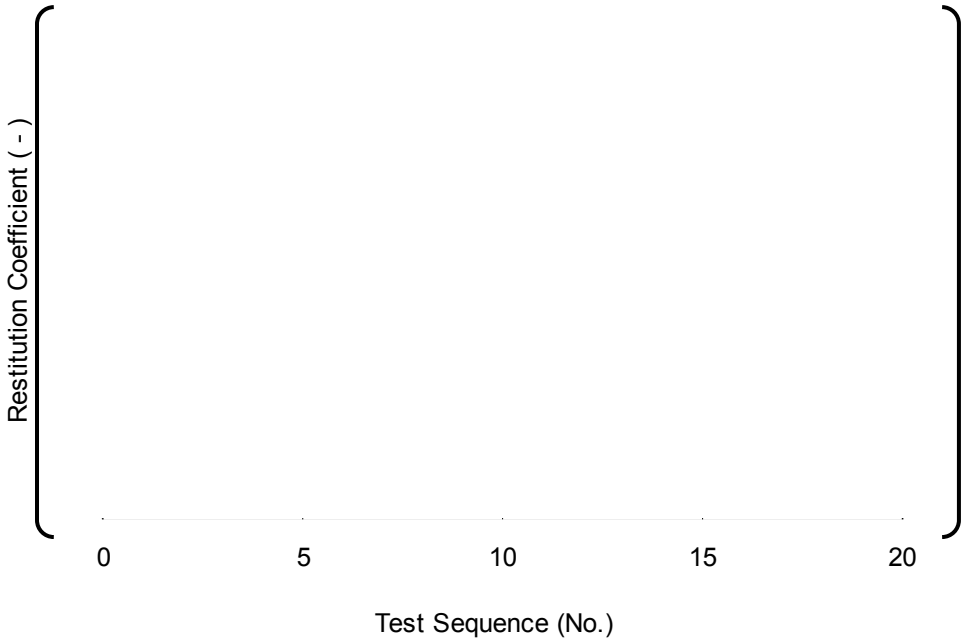

Figure A.3.1.2-3(b) Coefficient of Restitution (As-Built_6)

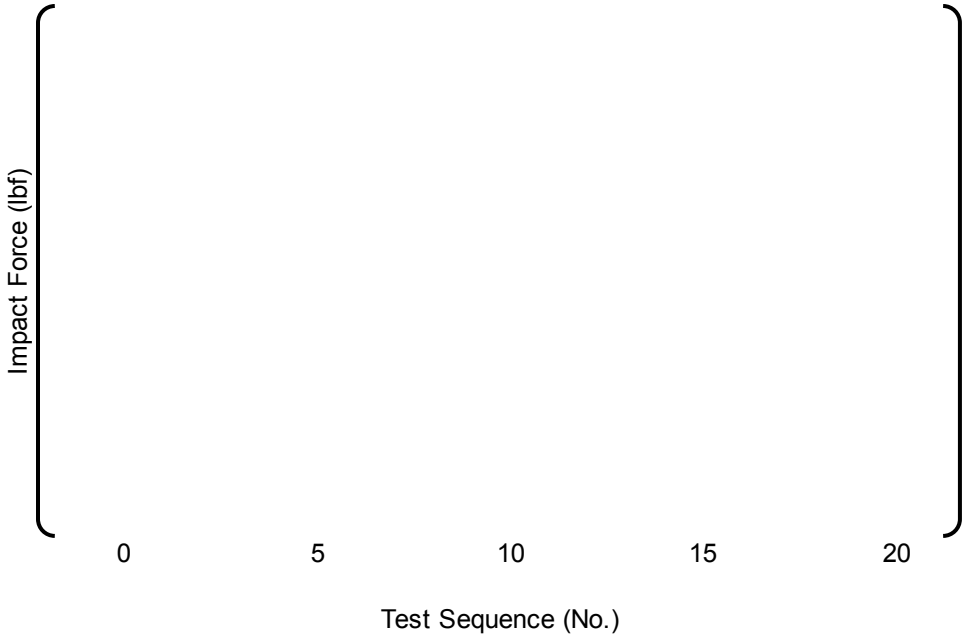

Figure A.3.1.2-4(a) Impact Force (Relaxed_7)

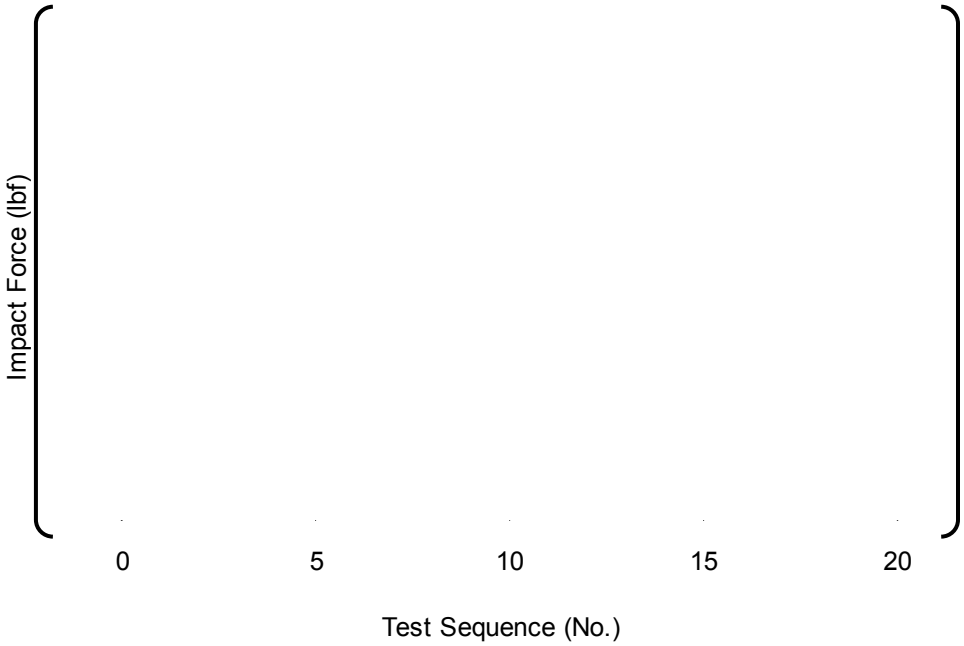

Figure A.3.1.2-4(b) Impact Force (Relaxed_8)

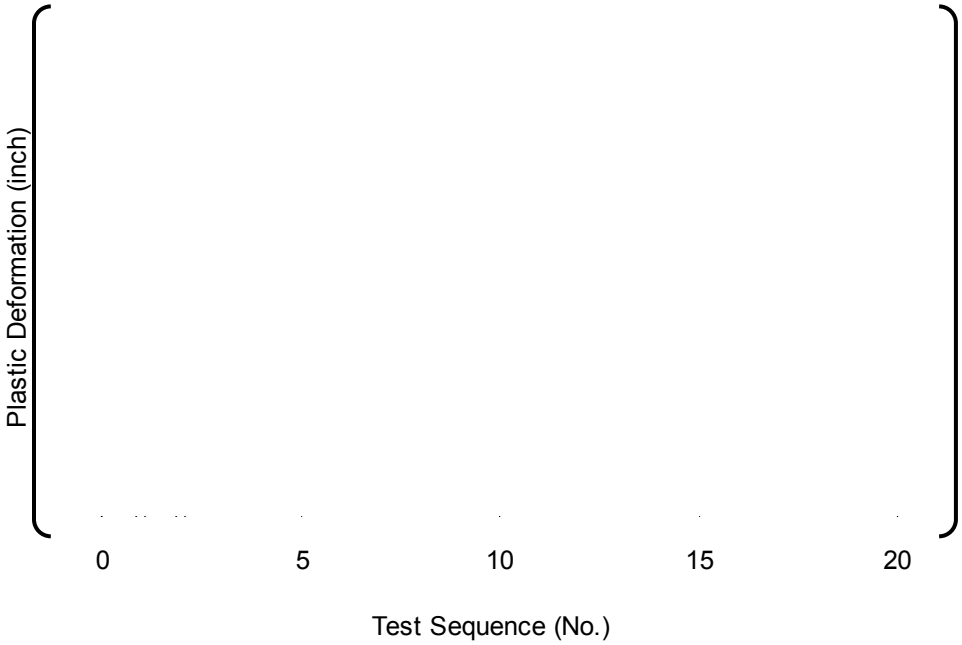

Figure A.3.1.2-5(a) Plastic Deformation (Relaxed_7)

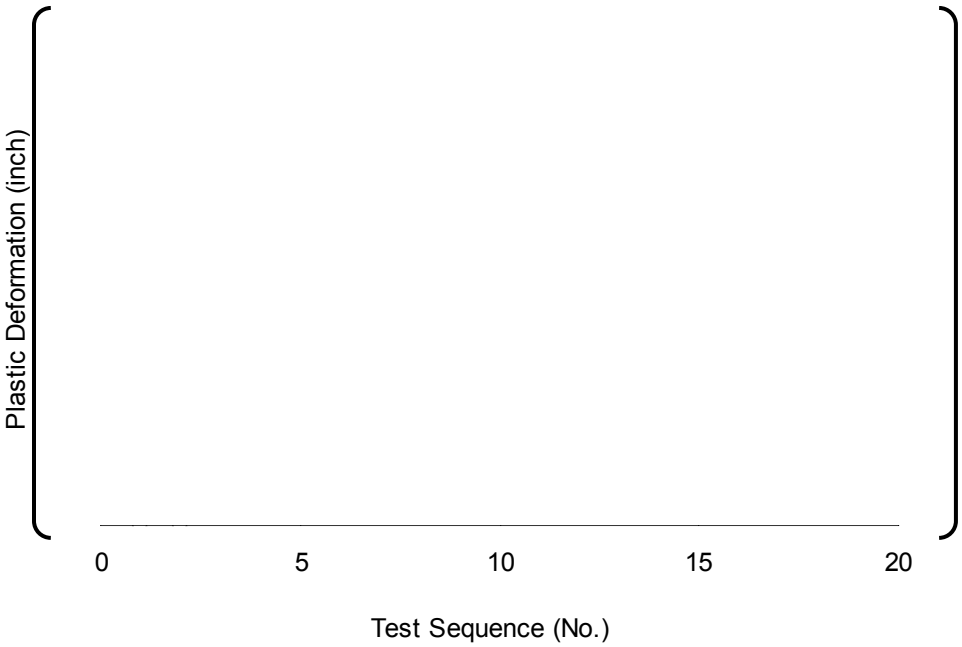

Figure A.3.1.2-5(b) Plastic Deformation (Relaxed_8)

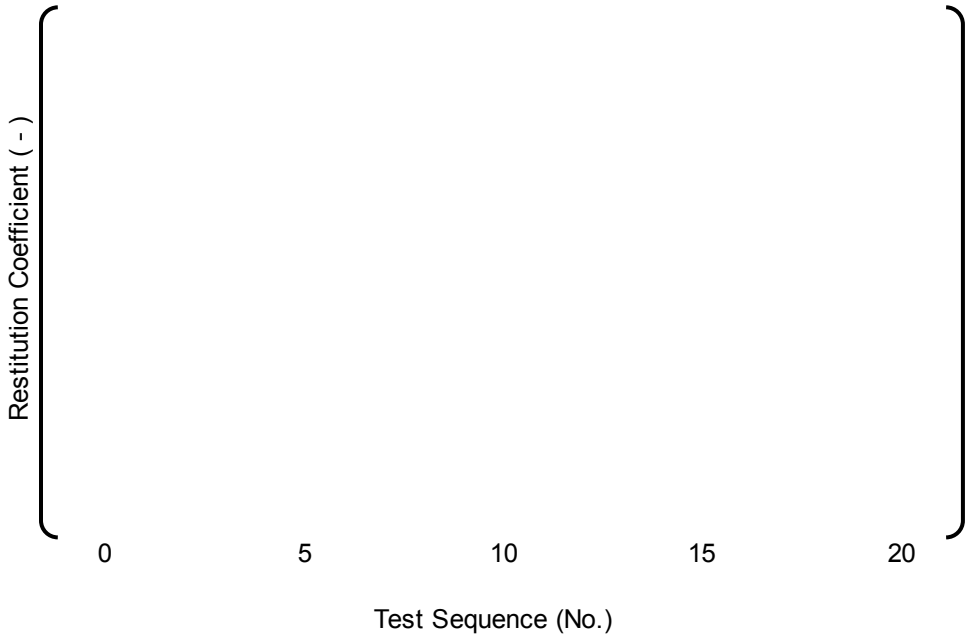

Figure A.3.1.2-6(a) Coefficient of Restitution (Relaxed_7)

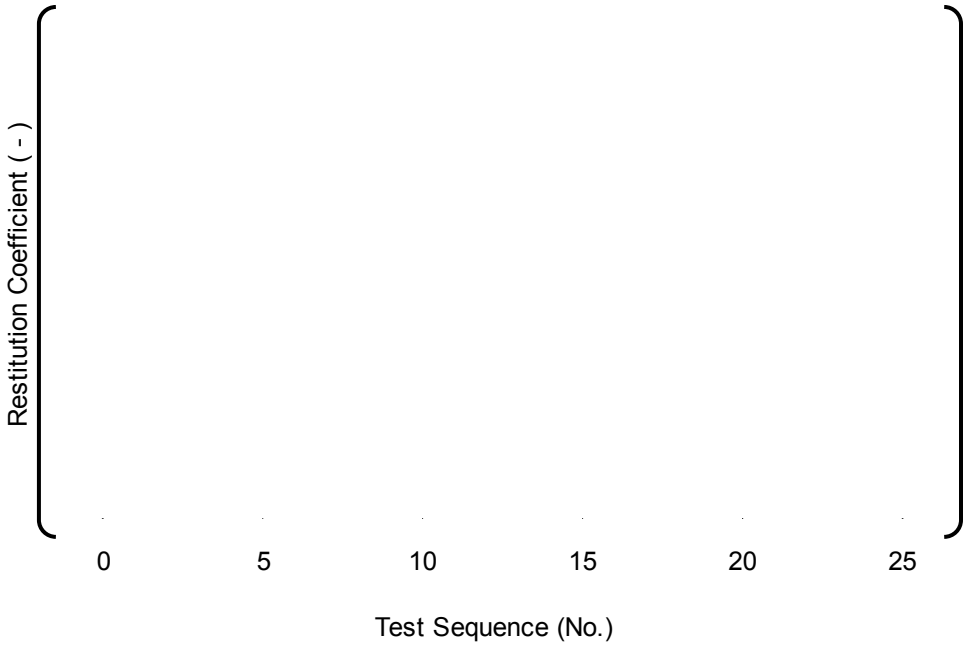

Figure A.3.1.2-6(b) Coefficient of Restitution (Relaxed_8)

A.3.2. Effect of Irradiation Brittleness

Brittleness of Zircaloy-4 due to irradiation and hydrogen absorption in a reactor may have an influence on grid spacer crush behavior. To investigate the influence, impact tests with hydrogen-absorbed grid spacers were performed.

A.3.2.1. Tested Grid Spacers

A grid spacer absorbed hydrogen in an autoclave filled with Lithium hydroxide solution as shown in Figure A.3.2.1-1. Although limiting of hydrogen absorption for the grid spacer is [ ] ppm, the grid spacer with [ ] ppm beyond the limit was prepared to consider more brittleness due to irradiation damage. The grid spacer cell sizes have been adjusted to give the gapped condition.

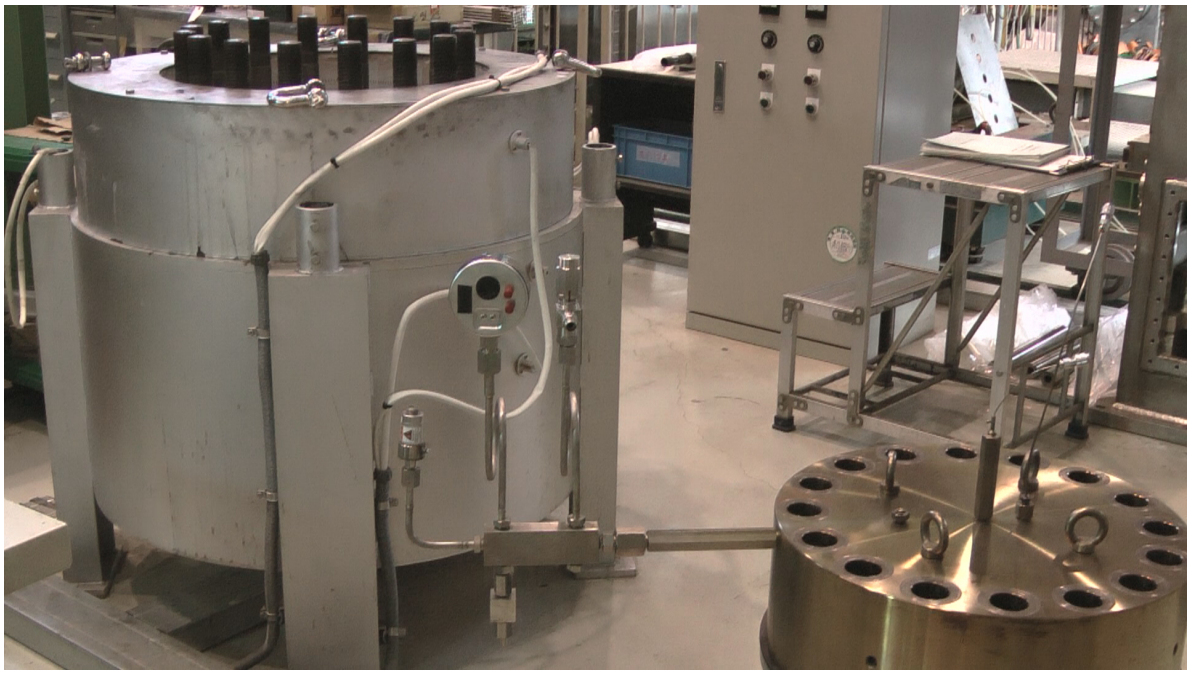

Figure A.3.2.1-1 Autoclave for Full-Sized Grid Spacer's Hydrogen Absorption

A.3.2.2. Test Procedure

Test procedure for the hydrogen-absorbed grid spacer is the same with that for the grid spacers with relaxed spring force described in Section A.3.1. Considering temperature in an operating reactor, temperature of the tested grid spacer is heated up to [ ] deg. F ([ ] deg. C). Short fuel rod claddings for 17x17 fuel assembly type are inserted in each cell of the hydrided grid spacer when the grid spacer is supplied to the impact test. While increasing the pendulum's initial swing-up angle, the impact test is repeatedly performed. The deformation progress after buckling of the hydrided grid spacer was also investigated to confirm the effect of the embrittlement on the crush behavior.

A.3.2.3. Test Results

(1) Buckling force

Figure A.3.2.3-1 shows relationship between impact force and impact velocity of the weight for the hydrided grid spacer. Two other grid spacers for as-built condition have been prepared and tested without short cladding to give the gapped condition. The test results are also included in Figure A.3.2.3-1.

As shown in Table A.3.2.3-1, buckling force of the hydrided grid spacer is [ ] lbf ([ ] kN) and is about [ ] % higher compared with that of [ ] lbf ([ ] kN) for as-built grid spacers. On the other hand, the dynamic stiffness of the hydrided grid spacer is [ ] lbf/inch ([ ] kN/mm) and is almost same with that of [ ] lbf/inch ([ ] kN/mm) for as-built grid spacers.

The thickness of the hydrided grid spacer strip is thicker compared with the one of as-built grid spacer strip due to the hydrogen absorption and it is considered that this difference of thickness of strip have large effect on the buckling force than on the dynamic stiffness. However, the increase of the buckling force due to hydrogen absorption is not considered in seismic analysis described in section A.4.0 for conservatism.

Table A.3.2.3-1 Buckling force and Dynamic Stiffness of the As-built and Hydrided Grid Spacers

Category		Buckling force		Dynamic Stiffness	
		(lbf)	(kN)	(lbf/inch)	(kN/mm)
As-built	As-built 7*				
	As-built 8*				
	Ave.				
Hydrided	Hydrided				

* Short claddings were not used in the tests.

(2) Plastic deformation

The deformation progression test has been performed using the same hydrided grid spacer to investigate the effect of material embrittlement on the deformation behavior. Figure A.3.2.3-2 shows the relationship between the plastic deformation and initial pendulum angle. The impact test results for Relaxed_8 grid spacer documented in Section A.3.1 are also shown in the same figure. The plastic deformation of the hydrided grid spacer is much less than that of the relaxed_8 grid spacer.

The grid spacer deformation modes are shown in Figure A.3.2.3-3 for the hydrided grid spacer and in Figure A.3.2.3-4 for Relaxed_8 grid spacer, respectively. The hydrided grid spacer showed “C-shaped” deformation mode and Relaxed_8 showed higher mode deformation shape. This difference in the deformation mode may cause the difference in plastic deformation progression between these grid spacers.

The hydrided grid spacer are deformed to [ ] inch ([ ] mm) and no crack due to brittleness is observed in grid spacer’s straps and welding points. The deformation range covers the maximum deformation of the grid spacer obtained by the FINDS analysis for the irradiated fuel assemblies in the reactor, which is described in section A.4.3.1.

Therefore, it is appropriate to use the FINDS in-elastic impact model, which is developed based on the test results for Relaxed_7 and 8, for seismic analysis described in section A.4.0.

Impact Force (lbf)

Impact Velocity of the Weight (inch/s)

Figure A.3.2.3-1 Impact Force versus Impact Velocity of As-built and Hydrided Grid spacers

Plastic Deformation (inch)

Initial Pendulum Angle (degree)

Figure A.3.2.3-2 Deformation Progression of As-built and Hydrided Grid spacers

Figure A.3.2.3-3 Top View of the Hydrogen-absorbed Grid Spacer (After the 5th Impact from 17 Degree)

Figure A.3.2.3-4 Top View of the Relaxed_8 Grid Spacer (After the 5th Impact Test from 14 Degree)

A.4.0 RESPONSE AND STRESS ANALYSIS OF IRRADIATED FUEL ASSEMBLY FOR SEISMIC AND LOCA EVENTS

A.4.1. Methodology for Irradiated Fuel Assembly Response and Stress Analysis for Seismic Conditions

The FINDS analysis model for the end of life fuel assembly is established by using the vibration behavior shown in Figure A.2.2-2 and the in-elastic impact model for the grid spacer with relaxed grid spring force described in Section A.3.0. The same procedure which is used for the as-built conditions in section 4.1 is applied to the evaluation for the irradiated condition, except for using the analytical model for the irradiated fuel assembly.

A.4.2. Methodology for Irradiated Fuel Assembly Response and Stress Analysis for LOCA Conditions

The same procedure used for the as-built conditions in section 4.2 is applied to the evaluation of the irradiated condition, except for using the analytical model for the irradiated fuel assembly.

A.4.3. Evaluation Results for the Irradiated Fuel Assembly Response and Strength for Combined Seismic and LOCA Events

A.4.3.1. Results of the Irradiated Fuel Assembly Horizontal Response Analysis

The FINDS response analyses for seismic and LOCA, in the horizontal direction have been performed using the following acceleration wave data obtained from the dynamic response analyses of the reactor vessel and core internals. They are the waves that resulted in the largest deflection for as-built conditions.

Safe shutdown earthquake (SSE):
- Medium 1

LOCA:
- CLB 14B 102%

All of the fuel assemblies in the array are assumed to be at the end of life condition for conservatism. The response analyses are performed for x and z direction individually, and the responses in the x and z directions are combined by the following equation for both seismic and LOCA, respectively:

$$D\max = \max\left(\sqrt{X_i(t)^2 + Z_j(t)^2}\right)$$

X(t), Z(t): Time history deflection of fuel assembly in x and z direction, respectively
i, j: Fuel assembly number in x and z direction and valid from 1 to 17, respectively.

The results for the maximum responses are shown in Table 4.3.1-1 for SSE and Table 4.3.1-2 for LOCA. The maximum deflections are [ ] inch ([ ] mm) for SSE and [ ] inch ([ ] mm) for CLB 14B 102% case.

The time history responses of the fuel assembly are shown in Figure A.4.3.1-1 for seismic and Figure A.4.3.1-2 for LOCA, respectively.

In the seismic evaluation the maximum deflection of the irradiated fuel assembly is almost ( ) times larger than for the as-built fuel assembly due to the large accelerations in conjunction with the grid spacer spring force relaxation. In the LOCA condition, the deflection is almost the same as the as-built result since the acceleration input is relatively small.

Table A.4.3.1-1 Irradiated Fuel Assembly Horizontal Response Analysis Results for Seismic (SSE Medium 1 Wave)

Wave	Units	SSE Medium 1
Maximum displacement	inch (mm)	
Time	s	
Fuel assembly number	-	
Grid number	-	
Maximum impact force*	lbf (N)	
Time	s	
Fuel assembly number **	-	
Grid number	-	
Maximum grid deformation	inch (mm)	

* Buckling force of the grid spacer is lbf ( )N in the FINDS code
** NR refers to the Neutron Reflector

Table A.4.3.1-2 Irradiated Fuel Assembly Horizontal Response Analysis Results for LOCA (CLB 14B 102% Wave)

Wave	Units	CLB 14B 102%
Fuel assembly array	-	17 x 17
Maximum displacement	inch (mm)	
Time	s	
Fuel assembly number	-	
Grid number	-	
Maximum impact force	lbf (N)	
Time	s	
Fuel assembly number *	-	
Grid number	-	

* NR refers to the Neutron Reflector

(a) x direction

(b) z direction

Figure A.4.3.1-1 (1) Irradiated Fuel Assembly Time History Response (SSE Medium 1)

(a) x direction

(b) z direction

Figure A.4.3.1-1 (2) Irradiated Fuel Assembly Time History Response (SSE Medium 1)

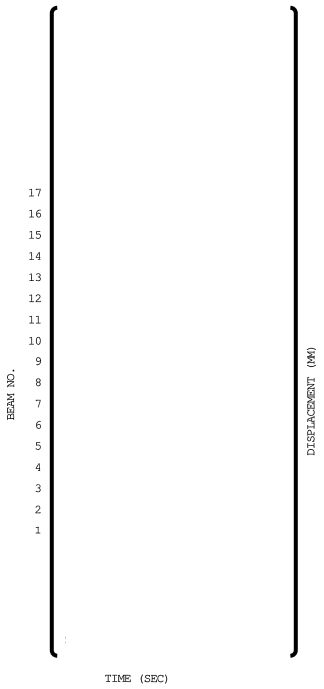

(a) x direction

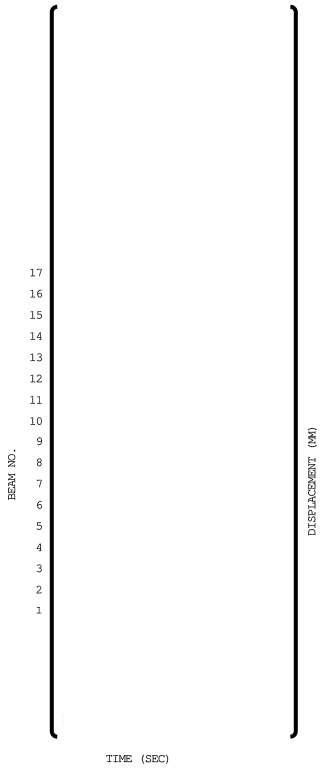

(b) z direction

Figure A.4.3.1-1 (3) Irradiated Fuel Assembly Time History Response (SSE Medium 1)

(a) x direction

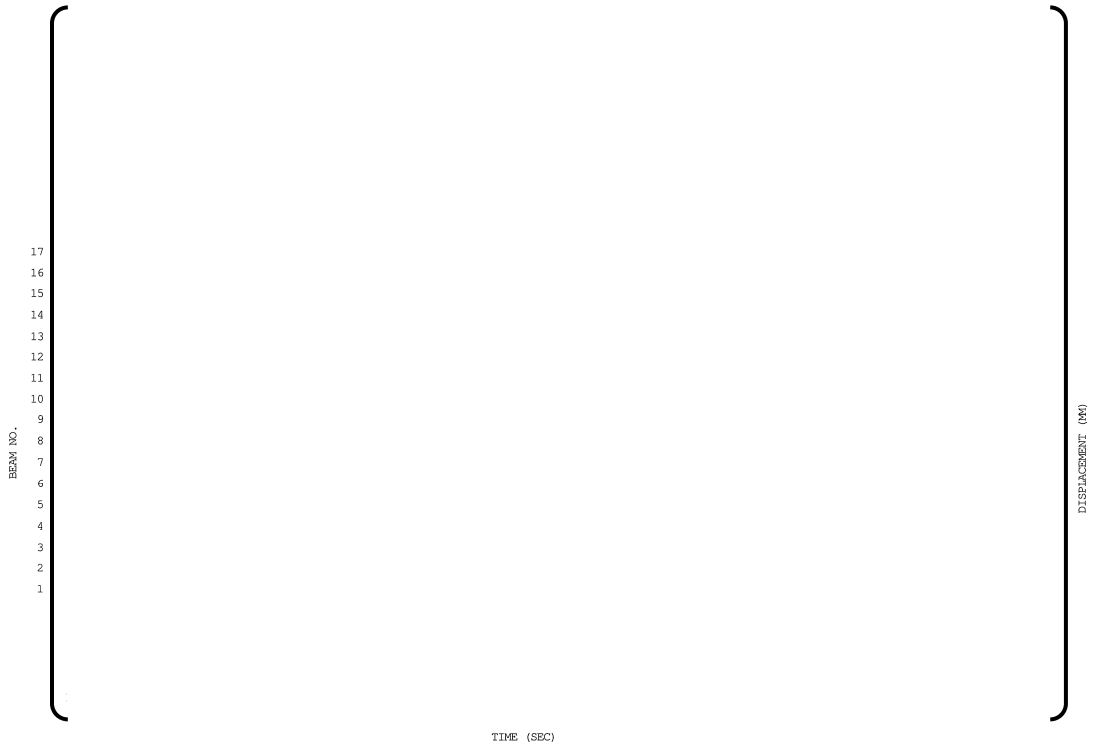

(b) z direction

Figure A.4.3.1-2 Irradiated Fuel Assembly Time History Response (CLB 14B 102%)

A.4.3.2. Irradiated Fuel Assembly Stress Evaluation Results under Safe Shutdown Earthquake and LOCA

The stresses due to SSE and LOCA are calculated individually and the combined stresses are calculated by the SRSS method. The results for the stresses are shown in Table A.4.3.2-1.

The integrity of the control rod guide thimble is maintained because the irradiated yield strength of Zr-4 is over 3 times the yield strength of non-irradiated Zr-4 as described in Appendix B of Reference A-5. Grid deformation occurs in the earthquake condition and this deformation causes the change in the alignment of the control rod guide thimble and fuel cladding. Therefore the stress caused by the grid deformation is considered and superimposed with the stress from the horizontal direction using the SRSS method.

The integrity of the other components is also shown to be maintained. [ ]

Table A.4.3.2-1 Stress Analysis Results for the Irradiated Fuel Assembly under Safe Shutdown Earthquake (Medium 1) and LOCA (CLB 14B 102%)

(a) Control rod guide thimble

Unit: ksi (MPa)

Stress Category	NO	SSE & LOCA	NO + SSE & LOCA	Acceptance limit at [ ] deg.F
Primary Membrane Stress				
Primary Membrane Stress + Primary Bending Stress				

* Stress due to vertical load
** Stress due to vertical load and horizontal displacement and distortion caused by the grid deformation
*** Increase of strength due to irradiation is considered.

(b) Top nozzle

Unit: ksi (MPa)

Stress Category	NO	SSE & LOCA	NO + SSE & LOCA	Acceptance limit at [ ] deg.F
Primary Membrane Stress + Primary Bending Stress				

* Stress due to the vertical load

(c) Bottom nozzle

Unit: ksi (MPa)

Stress Category	NO	SSE & LOCA	NO + SSE & LOCA	Acceptance limit at [ ] deg.F
Primary Membrane Stress + Primary Bending Stress				

* Stress due to the vertical load

(d) Grid spacer

Unit: inch (mm)

Maximum deformation	Acceptance limit
	No excessive deformation shall occur due to load during an accident.

(e) Buckling of control rod guide thimble

Unit: lbf (N)

Maximum force	Acceptance limit

A.5.0 INTEGRITY OF A ROD CLUSTER CONTROL ASSEMBLY CONSIDERING THE DEFLCETION OF AN IRRADIATED FUEL ASSEMLBY

Considering the deflection of the irradiated fuel assembly shown in Table A.4.3.1-1 for SSE and in Table A.4.3.1-2 for LOCA, the integrity of the RCCA is evaluated here.

Using the same procedure as described in Section 5 of the report, the stresses of the cladding and the top end plug of the control rod are calculated. The results are summarized as shown in Table A.5-1 to confirm that the integrity of the components is maintained.

Table A.5-1 Control Rod Stress Evaluation Results

(a) Cladding of control rod

Unit: ksi (MPa)

	Stress Category	Stress	Acceptance Limit @ 〔 〕 * deg.F(A-5)
Half inserted	Primary Membrane Stress	〔	〕
	Primary Membrane Stress +Primary Bending Stress		
Fully inserted	Primary Membrane Stress		
	Primary Membrane Stress +Primary Bending Stress		

* Obtained from thermal analysis performed for the control rod

(b) Top end plug of control rod (reduced diameter portion)

Unit: ksi (MPa)

	Stress Category	Stress	Acceptance Limit @ 〔 〕 ** deg.F(A-5)
Half inserted	Primary Membrane Stress	〔	〕
	Primary Membrane Stress +Primary Bending Stress		
Fully inserted	Primary Membrane Stress		
	Primary Membrane Stress +Primary Bending Stress		

** Outlet temperature of the core

A.6.0 CONCLUSION

The effects of grid spacer spring relaxation due to irradiation on the fuel assembly's vibration behavior and the grid spacer crush behavior were discussed in this appendix. Considering these effects, the dynamic response analyses have been performed and the integrity of the fuel assembly has been evaluated for the responses to confirm that the integrity is maintained. Also, it has been confirmed that the integrity of the rod cluster control assembly is maintained considering the deflection of the irradiated fuel assembly.

The effect of the reduced ductility of the grid spacer material (due to irradiation hardening) on the grid spacer's crush strength and deformation behavior was also described in this Appendix and it was shown that the ductility does not make the crush behavior worse.

A.7.0 REFERENCES

(A-1) MHI's Responses to the NRC's Requests for Additional Information on Topical Report MUAP-07034-P(0) "FINDS: Mitsubishi PWR Fuel Assemblies Seismic Analysis Code", UAP-HF-08139-P (Propiretary) and UAP-HF-08139-NP (Non-Proprietary), August 2008

(A-2) Response for Quenstion 5 in MHI's Responses to the NRC's Requests for Additional Information on Topical Report MUAP-07034-P(0) "FINDS: Mitsubishi PWR Fuel Assemblies Seismic Analysis Code", UAP-HF-08309-P (Proprietary) and UAP-HF-08309-NP (Non-Proprietary)

(A-3) U.S. Nuclear Regulatory Commission, Standard Review Plan (NUREG-0800) Section 4.2, March 2007

(A-4) "FINDS: Mitsubishi PWR Fuel Assemblies Seismic Analysis Code", MUAP-07034-P (Proprietary) and MUAP-07034-NP (Non-Proprietary), March 2008

(A-5) "US-APWR Fuel System Design Evaluation", MUAP-07016-P (Proprietary) and MUAP-07016-NP (Non-Proprietary), Feb 2008

Appendix B

PARAMETRIC STUDY ON THE SENSITIVITY OF FINDS INPUT UNCERTAINTY ON FINDS ANASLYSIS RESULTS

March 2009

Table of Contents

List of Tables

List of Figures

B.1.0 INTRODUCTION

The fuel assembly's material properties, amplitude-dependent frequency and damping are used for the input to the FINDS code. The effect of the uncertainties associated with material properties, frequency and damping is confirmed in Reference B-1.

A parametric study is performed to determine the sensitivity of FINDS results to material properties, frequency and damping variations by using the representative US-APWR plant acceleration wave. This parametric study is documented in this Appendix.

The variation of Young's modulus is considered as the uncertainty associated with material properties in Reference B-1, while the variations in input amplitude and frequency of 10 percent respectively can be considered as the uncertainty evaluation in compliance with the Appendix A Section II.3 of Reference B-2.

B.2.0 EFFECT OF FINDS INPUT UNCERTAINTY

B.2.1 Effect of Input Acceleration Amplitude Uncertainty

In this section, the effect of the variation in input acceleration amplitude of 10 percent is discussed consistent with Appendix A Section II.3 of Reference B-2.

The FINDS dynamic analysis is performed using 1.1 times the original Medium 1 wave amplitude and the analysis results are shown in Table B.2.1-1. The analysis is performed using the Medium 1 wave which gives the maximum fuel assembly deflection. The results are compared with the original result in the x and the z direction respectively to quantify the effect of the amplitude variation.

Since a 10 percent change in input amplitude only resulted in a [ ] percent increase (compared to the allowable of 15%) in the fuel assembly response, acceptable model sensitivity exists. Therefore no sensitivity factor due to input acceleration amplitude variation needs to be applied to the fuel assembly analysis results.

The variation in plastic deformation is larger compared with the input acceleration amplitude variation, however there is a negligible effect on the fuel assembly maximum deflection because the additional grid deformation is a negligible contribution to the fuel assembly's total deflection which is most important in evaluating the fuel assembly's integrity.

Table B.2.1-1 Sensitivity Result for the Input Acceleration Amplitude (SSE Medium 1 Wave)

Wave	Units	SSE Medium1			
Variation	-	amplitude of 10 percent		standard	
Direction	-	x	z	x	z
Maximum displacement	inch (mm)				
Time	s				
Fuel assembly number	-				
Grid number	-				
Maximum Impact force*	lbf (N)				
Time	s				
Fuel assembly number **	-				
Grid number	-				
Maximum grid plastic deformation	inch (mm)				
Fuel assembly number	-				
Grid number	-				

* Buckling force of the grid spacer is [ ] lbf ([ ])N in the FINDS code
** NR refers to the Neutron Reflector

B.2.2 Effect of Frequency Uncertainty

The variation in amplitude-dependent frequency is considered in Reference B-1, while the variations in input amplitude and frequency of 10 percent respectively can be considered as the uncertainty evaluation in compliance with Appendix A Section II.3 of Reference B-2.

In this section, the effect of the variation in input acceleration frequency of ± 10 percent is discussed. The impact of variations in the fuel assembly amplitude-dependent frequency relationship is close to the same magnitude as the variations in the input acceleration frequency.

The sensitivity analysis of the input acceleration frequency is performed using 1.1 and 0.9 times the original Medium 1 wave period and the results are shown in Table B.2.2-1 for the x and z direction, the same way as in section B.2.1.

Since a ± 10 percent change in frequency only resulted in a [ ] percent increase in the fuel assembly response, acceptable model sensitivity exists. Therefore no sensitivity factor due to input frequency variation needs to be applied to the fuel assembly response standard analysis results.

The variation in plastic deformation is larger compared with the input acceleration frequency variation, however there is a negligible effect on the fuel assembly maximum deflection because the additional grid deformation is a negligible contribution to the fuel assembly's total deflection, which is most important in evaluating its integrity.

Table B.2.2-1 Sensitivity Result for the Input Acceleration Frequency (SSE Medium 1 Wave)

Wave	Units	SSE Medium 1					
Variation	-	frequency of - 10 percent		frequency of + 10 percent		standard	
Direction	-	x	z	x	z	x	z
Maximum displacement	inch (mm)						
Time	s						
Fuel assembly number	-						
Grid number	-						
Maximum Impact force*	lbf (N)						
Time	s						
Fuel assembly number **	-						
Grid number	-						
Maximum grid plastic deformation	inch (mm)						
Fuel assembly number	-						
Grid number	-						

* Buckling force of the grid spacer is [ ] lbf ([ ])N in the FINDS code
** NR refers to the Neutron Reflector

B.2.3 Effect of the Damping Uncertainty

In this section, the effect of the variation in amplitude-dependent damping of 10 percent, using the representative US-APWR plant acceleration wave, is discussed. This variation is also considered in Reference B-1.

The comparison of the amplitude dependency of damping between the models with standard damping and with the 10 percent reduced damping is shown in Figure B.2.3-1. The reduction of 10 percent in damping is obtained by using the 0.9 times the original damping factor.

The FINDS analysis results, using the models with the lower amplitude dependence of damping, are shown in Table B.2.2-1. The analyses are performed for the Medium 1 wave as in the previous section.

Since a 10 percent change in damping only resulted in a [ ] percent increase in the fuel assembly response, no significant feedback exists. Therefore no sensitivity factor due to input frequency variation needs to be applied to the fuel assembly response standard analysis results.

The variation in plastic deformation is larger compared with the damping variation, however there is a negligible effect on the fuel assembly maximum deflection because the additional grid deformation is a negligible contribution to the fuel assembly's total deflection, which is most important in evaluating its integrity.

Table B.2.3-1 Sensitivity Result for the Damping (SSE Medium 1 Wave)

Wave	Units	SSE Medium 1			
Variation	-	damping of 10 percent		standard	
Direction	-	x	z	x	z
Maximum displacement	inch (mm)				
Time	s				
Fuel assembly number	-				
Grid number	-				
Maximum Impact force*	lbf (N)				
Time	s				
Fuel assembly number **	-				
Grid number	-				
Maximum grid plastic deformation	inch (mm)				
Fuel assembly number	-				
Grid number	-				

* Buckling force of the grid spacer is [ ] lbf ([ ])N in the FINDS code
** NR refers to the Neutron Reflector

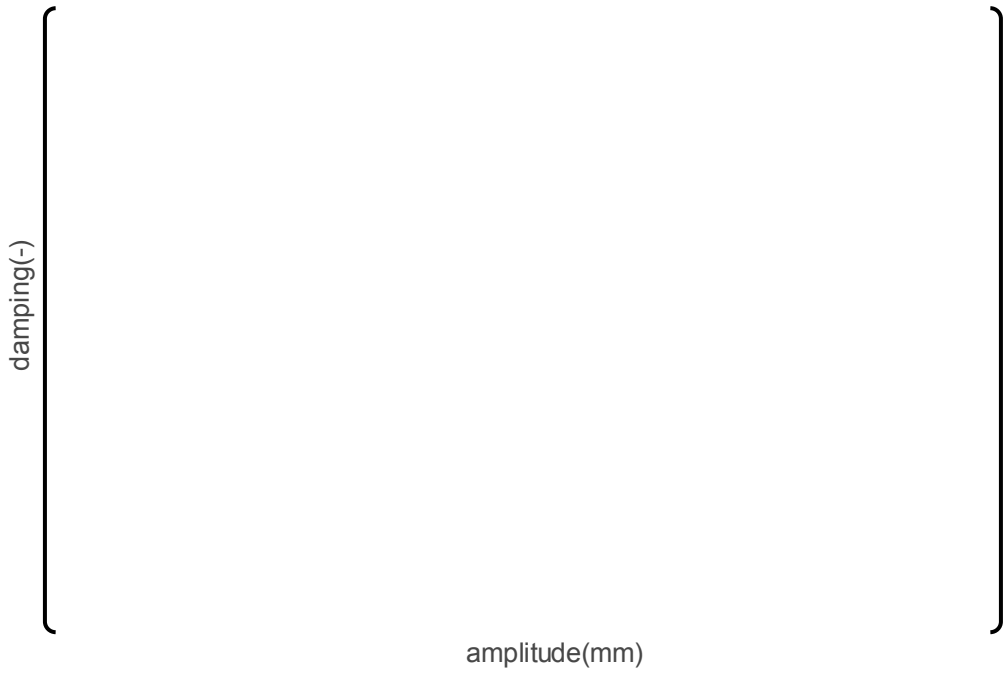

Figure B.2.3-1 Comparison of Amplitude Dependent of Damping (Hot Water Condition)

B.3.0 CONCLUSION

The fuel assembly's material properties, amplitude-dependent frequency and damping are used as the input to the FINDS code. The effect of the input uncertainties is discussed and the sensitivity of these uncertainties when using the representative US-APWR plant acceleration wave is confirmed to be less than the allowable variation of 15 percent.

B.4.0 Reference

(B-1) Response for Question 3 in MHI's Responses to the NRC's Requests for Additional Information on Topical Report MUAP-07034-P(0) "FINDS: Mitsubishi PWR Fuel Assemblies Seismic Analysis Code", UAP-HF-08309-P (Proprietary) and UAP-HF-08309-NP (Non-Proprietary)

(B-2) U.S. Nuclear Regulatory Commission, Standard Review Plan (NUREG-0800) Section 4.2, March 2007